



National Library  
of Canada

Bibliothèque nationale  
du Canada

Canadian Theses Service

Services des thèses canadiennes

Ottawa, Canada  
K1A 0N4

## CANADIAN THESES

## THÈSES CANADIENNES

### NOTICE

The quality of this microfiche is heavily dependent upon the quality of the original thesis submitted for microfilming. Every effort has been made to ensure the highest quality of reproduction possible.

If pages are missing, contact the university which granted the degree.

Some pages may have indistinct print especially if the original pages were typed with a poor typewriter ribbon or if the university sent us an inferior photocopy.

Previously copyrighted materials (journal articles, published tests, etc.) are not filmed.

Reproduction in full or in part of this film is governed by the Canadian Copyright Act, R.S.C. 1970, c. C-30.

**THIS DISSERTATION  
HAS BEEN MICROFILMED  
EXACTLY AS RECEIVED**

### AVIS

La qualité de cette microfiche dépend grandement de la qualité de la thèse soumise au microfilmage. Nous avons tout fait pour assurer une qualité supérieure de reproduction.

S'il manque des pages, veuillez communiquer avec l'université qui a conféré le grade.

La qualité d'impression de certaines pages peut laisser à désirer, surtout si les pages originales ont été dactylographiées à l'aide d'un ruban usé ou si l'université nous a fait parvenir une photocopie de qualité inférieure.

Les documents qui font déjà l'objet d'un droit d'auteur (articles de revue, examens publiés, etc.) ne sont pas microfilmés.

La reproduction, même partielle, de ce microfilm est soumise à la Loi canadienne sur le droit d'auteur, SRC 1970, c. C-30.

**LA THÈSE A ÉTÉ  
MICROFILMÉE TELLE QUE  
NOUS L'AVONS REÇUE**

**Ultimate Bearing Capacity of Triangular  
Shell Strip Footings on Sand**

**Mohamed Abd El-Rahman**

**A Thesis  
in  
The Department  
of  
Civil Engineering**

**presented in Partial Fulfillment of the Requirements  
for the Degree of Master of Engineering at  
Concordia University  
Montréal, Québec, Canada**

**August 1987**

**© Mohamed Abd El-Rahman, 1987.**


Permission has been granted to the National Library of Canada to microfilm this thesis and to lend or sell copies of the film.

The author (copyright owner) has reserved other publication rights, and neither the thesis nor extensive extracts from it may be printed or otherwise reproduced without his/her written permission.

L'autorisation a été accordée à la Bibliothèque nationale du Canada de microfilmer cette thèse et de prêter ou de vendre des exemplaires du film.

L'auteur (titulaire du droit d'auteur) se réserve les autres droits de publication; ni la thèse ni de longs extraits de celle-ci ne doivent être imprimés ou autrement reproduits sans son autorisation écrite.

ISBN 0-315-37086-6



**CONCORDIA UNIVERSITY**  
**Division of Graduate Studies**

This is to certify that the thesis prepared

By: \_\_\_\_\_

Entitled: \_\_\_\_\_

\_\_\_\_\_

and submitted in partial fulfillment of the requirements for the degree of

\_\_\_\_\_

complies with the regulations of this University and meets the accepted standards  
with respect to originality and quality.

Signed by the final examining committee:

\_\_\_\_\_ Chair

\_\_\_\_\_

\_\_\_\_\_

\_\_\_\_\_

\_\_\_\_\_

\_\_\_\_\_ Supervisor

Approved by \_\_\_\_\_  
Chairman of department or Graduate  
Program Director

\_\_\_\_\_ 19 \_\_\_\_\_

\_\_\_\_\_ Dean of Faculty

## ABSTRACT

### Ultimate Bearing Capacity of Triangular Shell Strip Footings on Sand

Mohamed M. Abd El-Rahman

Shell foundations are of recent origin and as such there is no theoretical study in literature available about their ultimate bearing capacity and settlement characteristics. However, experimental investigations showed that the use of shell foundation leads to considerable savings in construction materials, higher bearing capacity, better settlement characteristics and greater resistance to lateral loads, all of which provide viable alternative to the conventional flat foundation. Recent applications of shell foundations have been demonstrated in high-rise buildings, chimneys, silos and tele-communication towers.

In the present study triangular shell strip footing was investigated experimentally and theoretically. Experimental investigations on five strip foundation models were conducted in order to study the effect of the peak angle " $\theta$ " of the triangular shell strip footing on the ultimate bearing capacity. Two embedment conditions, namely surface and buried, were conducted on each model. The ultimate bearing capacity increased up to thirty-six percent by using triangular shell footings instead of the conventional flat foundation.

A theoretical study on triangular strip footings has been developed by applying the theory of plasticity. Three new coefficients ( $N_{ct}$ ,  $N_{qt}$  and  $N_{\gamma t}$ ) have been introduced to modify the Terzaghi's bearing capacity coefficients ( $N_c$ ,  $N_q$  and  $N_\gamma$ ). The new factors depend on the peak angle of the foundation " $\theta$ " and angle of internal friction of sand " $\phi$ ". A comparison between the experimental and the theoretical results showed good agreement. Shell foundations should be encouraged to come into wider use in the future, wherever the scope exists for employing them effectively and feasibly.

*To my parents, my fiancée and my country*

## ACKNOWLEDGEMENTS

The author gratefully acknowledges the invaluable guidance and cooperation of Professor A.M. Hanna, under whose supervision this work was carried out. The author is also grateful to Professor N.S. Verma, co-supervisor, for his many helpful suggestions and useful discussions. Many thanks go out to Messrs Moustafa Abumangel and Hisham Derbala for their help in the laboratory works, and to Ms. Teresa Rego for her judicious typing of the entire thesis. The author is grateful to the National Science and Engineering Research Council of Canada for the financial support.

## TABLE OF CONTENTS

Page

Abstract.....	iii
Dedication.....	iv
Acknowledgements.....	v
Table of Contents.....	vi
List of Figures.....	viii
List of Tables.....	x
Notations.....	xi

### CHAPTER 1 : INTRODUCTION

1.1 Foundation Engineering Design.....	1
1.2 Shell Foundations.....	2

### CHAPTER 2 : LITERATURE REVIEW

2.1 General.....	4
2.2 Soil Pressure Distribution.....	7
2.3 Slip-lines Fields and General Bearing Capacity Equation.....	10

### CHAPTER 3 : EXPERIMENTAL INVESTIGATION

3.1 General.....	15
3.2 Description of the Foundation Models.....	15
3.3 Description of the Experimental Set-up.....	16
3.4 Experimental Procedure and Results.....	25



## CHAPTER 4 : ANALYSIS OF THE THEORITICAL MODEL

4.1 General.....	38
4.2 Upper Bound Solution for Rough Triangular Foundation on Weightless Soil .....	43
4.3 Bearing Capacity of Triangular Foundation on Soil having Weight .....	49
4.4 Calculations of the Ultimate Load of the Foundation Models .....	57

## CHAPTER 5 : CONCLUSION AND RECOMMENDATIONS.....61

## LIST OF REFERENCES.....63

## Appendix "A" : LABORATORY TEST RESULTS

Sheet 1 : Load versus Settlement- Surface loading.....	66
Sheet 2 : Load versus Settlement- Buried loading.....	67

## LIST OF FIGURES

	Page
Figure 2.1 Shell Foundation of T.V. tower- Stuttgart, West Germany.....	5
Figure 2.2 Shell Foundation of Telex tower -Hamburg, West Germany.....	5
Figure 2.3 Soil Pressure Distribution on the Lower Shell.....	8
Figure 2.4 Curvature of the Upper Shell and Shear Wall.....	8
Figure 2.5 Soil Pressure Distribution in Axial direction.....	9
Figure 2.6 Soil Pressure Distribution in Radial direction.....	9
Figure 2.7 Typical Rupture Surfaces beneath a foundation at Failure.....	11
Figure 3.1 Cross Section of the Foundation Models.....	17
Figure 3.2 End View of the Foundation Models.....	18
Figure 3.3 Top View of the Triangular Models.....	18
Figure 3.4 Overall View of the Sand Spreading Enclosure.....	20
Figure 3.5 The Testing Tank during Sand Spreading Operation.....	21
Figure 3.6 The Testing Tank with Foundation Model on Top.....	22
Figure 3.7 The Testing Tank hungup with Straps.....	23
Figure 3.8 The Testing Tank on the Platform of The Compression Machine....	24
Figure 3.9 Overall View of the Compression Machine.....	26
Figure 3.10 Close-up View during Loading Test.....	27
Figure 3.11 Sieve Analysis.....	28
Figure 3.12 Plot of the Unit Weight versus The Height of Drop.....	29
Figure 3.13 Direct Shear Test Results.....	31
Figure 3.14 Angle of Internal Friction of Sand " $\Phi$ ".....	31
Figure 3.15 Load versus Settlement- Surface Loading.....	35
Figure 3.16 Load versus Settlement- Buried Loading.....	36

	Page
Figure 4.1 Stress/Strain Relationships.....	40
Figure 4.2 Stress Components in Cartesian Coordinates.....	40
Figure 4.3 A Triangular Rough Foundation on Weightless Soil .....	44
Figure 4.4 Shell Factor " $F_c$ " .....	52
Figure 4.5 Shell Factor " $F_q$ " .....	53
Figure 4.6 Design Chart : Coefficient " $N_{ct}$ " for Triangular Strip Footing.....	54
Figure 4.7 Design Chart : Coefficient " $N_{qt}$ " for Triangular Strip Footing.....	55
Figure 4.8 Design Chart : Coefficient " $N_{yt}$ " for Triangular Strip Footing.....	56
Figure 4.9 Comparison between The Theoretical and Experimental Results.....	60

## LIST OF TABLES

	Page
TABLE 2.1 Comparison between Different Types of Foundation .....	6
TABLE 2.2 Values of Coefficient $N_\gamma$ by Different Methods.....	14
TABLE 3.1 Ultimate Load for the Foundation Models.....	37
TABLE 4.1 Theoretical Results for the Ultimate Load for the Foundation Models.....	58
TABLE 4.2 Increase in the Ultimate Bearing Capacity of the Triangular Shell Models relative to the Flat One.....	58
TABLE 4.3 Comparison Between the Experimental and Theoretical Results for Case of Surface Loading.....	59
TABLE 4.4 Comparison Between the Experimental and Theoretical Results for Case of Buried Loading.....	59

## NOTATIONS

- $B$  : Width of foundation
- $c$  : Apparent cohesion (in terms of total stress)
- $c'$  : Apparent cohesion (in terms of effective stress)
- $D$  : Depth of foundation
- $f$  : Plastic potential function
- $F_c$  : Shell factor for changing bearing capacity coefficient  $N_c$
- $F_q$  : Shell factor for changing bearing capacity coefficient  $N_q$
- $L$  : Length of foundation
- $M$  : Bending moment
- $N$  : Normal force
- $N_c$  : Terzaghi's bearing capacity coefficient due to cohesion
- $N_q$  : Terzaghi's bearing capacity coefficient due to surcharge
- $N_\gamma$  : Terzaghi's bearing capacity coefficient due to friction
- $N_{ct}$  : Bearing capacity coefficient for triangular shell strip footings due to cohesion
- $N_{qt}$  : Bearing capacity coefficient for triangular shell strip footings due to surcharge
- $N_{\gamma t}$  : Bearing capacity coefficient for triangular shell strip footings due to friction
- $q$  : Soil pressure
- $q_0$  : Surcharge load
- $q_u$  : Ultimate bearing capacity of foundation
- $u$  : Pore water pressure
- $t$  : Time
- $V$  : Velocity

$X$  : Body force per unit volume acting in "x" direction

$Z$  : Body force per unit volume acting in "z" direction

$\alpha$  : Angle

$\beta$  : Incremental change in angle  $\alpha$

$\theta$  : Peak angle of triangular shell foundation

$\epsilon_n^P$  : Plastic longitudinal strain rate

$\gamma^P$  : Plastic shear strain rate

$\phi$  : Angle of internal friction of sand (in terms of total stress)

$\phi'$  : Angle of internal friction of sand (in terms of effective stress)

$\sigma_n$  : Normal stress at failure

$\tau$  : Shear stress components

$\tau_f$  : Shear strength

$\xi$  : Angle

## CHAPTER 1

### INTRODUCTION

#### 1.1 Foundation Engineering Design

The designer of a foundation must ensure that the foundation meets basic considerations of safety, dependability, functional utility, and economy. Specifically, the foremost of these are the requirements of tolerable settlements, and safety against failure.

The requirement of tolerable settlement concerns with total and differential settlements of all foundations under the planned structure. The differential settlements must be limited to avoid structural distress or excessive tilting of the superstructure, and often to respect the serviceability requirements of the superstructure. The total settlements must be limited because they invariably induce differential settlements, even in apparently homogenous soil conditions.

The requirement of safety against failure is centered around two principal kinds of failure that may be of concern in design: the structural failure of the foundation and the bearing capacity failure of the supporting soil. The structural failure of the foundation may occur if the foundation itself is not properly designed to sustain the imposed stresses or if no enough site investigations were conducted. Catastrophic collapse of the soil beneath the foundation can be occurred if the shear strength is inadequate to support the applied load.

Research works have been established on different foundation configurations and it was discovered from experimental results that these foundations have higher bearing capacity and better settlement characteristics than the conventional flat foundation (1).

These new models are called shell foundations. Different types of shell foundations include: triangular, conical, spherical, cylindrical, parabolic, hyperbolic and hyperbolic-paraboloid. This study is devoted to the analysis of the ultimate bearing capacity of the triangular shaped shell foundation acting as strip footings on frictional soil.

## 1.2 Shell Foundations

Shells have staged an entry into foundation engineering in the mid-fifties in Mexico (1), and like many other design components and techniques in Civil Engineering, their application preceded research. Since then the subject has been investigated particularly in India, the Soviet Union, West Germany, China and Canada (Concordia University).

The analysis of shell foundation, until now, was based on the assumption of uniform soil pressure distribution acting normal to the surface of the shell. This is true only for plastic soils of liquid character, and does not agree with the actual behaviour of the foundation soil in the majority of the cases.

There are three practical factors which may be considered in comparing shell foundations with flat foundations. First, to excavate and shape the ground to the contours required for a shell foundation will be more difficult and more costly than to excavate for a comparable flat foundation. However, with the now commonly used of hydraulic powered excavators which are capable of removing material much faster and to much more accurate tolerances than the older "Cable and Gear" powered machines, the future prospects for the excavation phase of installing shell foundations is looking more attractive. In addition the use of Robots on construction sites, now in the experimental stage, which can be preprogrammed for excavation to very accurate shapes, elevations and tolerances, which quite conceivably in the near future can make the excavation of shell foundations a routine and economical operation.

The second consideration is the method of construction of the foundation itself. In recent years there has been rapid advance in the efficiency and reliability of the technology connected with constructing and assembling precast concrete sections. This has already been adapted to the flat foundation type, and the potential is there for footings of different shapes as well.



The third consideration for choosing the required type of foundation for any structures is its technical behaviour. From practical experience (11) shell foundations have been found to have more ability to resist lateral forces produced due to wind loads or earthquakes, making them very effective in the case of high-rise buildings, chimneys and tele-communication towers than their flat equivalents. Their higher bearing capacity and better settlement characteristics with respect to the conventional flat foundations are additional aspects for the technical behaviour consideration.

From the three previous considerations it can be argued that the attributes associated with shell foundations would appear to make them ideally suited for use in high-rise buildings in crowded city conditions. Since the desired bearing capacity can be achieved from shell footings with less horizontal area than that required for the flat footings, this circumstance can make purchasing land for a proposed building more economical. This same consideration where less land area is required because of reduced footing area can also prove to be extremely helpful when attempting to fit as large a building as possible onto a certain size of land. It follows from this that less space required for perimeter foundations makes the task of locating a downtown high-rise building next to an existing building much simpler. In this situation, the use of shell foundations can possibly negate the need for eccentric footing loading required if flat footings were used, where a certain minimum width could not be centered directly under the loading points due to the lack of perimeter space outside the wall line of the building. Shell foundations could also be considered advantageous in a situation where ample space for flat footings is not a problem, but where the settlement allowed is very minimal, for here shell foundations with the same horizontal area as flat type would have considerably more bearing capacity, and thus better settlement characteristics, which can possibly negate the need for either raft or pile foundations.

## CHAPTER 2

### LITERATURE REVIEW

#### 2.1 General

No theoretical work on the ultimate bearing capacity and settlement of shell foundations has been reported in the literature, most of the work in this area has been done experimentally (1 & 9) to show the economy of using shells as foundations.

The subject having gone into fairly extensive literature and code of practice in India, emphasis is laid only on the aspect of the ultimate strength of the shell itself.

Shell foundations have been used for tele-communication towers in West Germany. Stuttgart T.V. tower, which was constructed in 1956 of height 211 meters, shown in Figure 2.1 and Figure 2.2 shows the 271 meters Hamburg Telex tower, which was built in 1967.

During the last 10 years researchers in China (9) reported some experimental results related to the ultimate strength analysis and construction techniques for shell foundation. They used the term of "empty-shell foundations" for these foundations which are made of two cones, one is facing up and the other down. They introduced a feasibility study for different types of foundation for chimneys on different soil conditions to show the economic advantages of using empty - shell foundation with comparing to other types of foundation, the results of this study summarized in Table 2.1 indicated a material saving of about 50 to 80 percent of concrete and about 40 to 70 percent of steel reinforcement. The technical advantages of shell foundations have been summarized as follows :

1. The load coming from the body of the shear wall transferred from a small area to a bigger area which leads that internal forces due to the wind loads (which is governing in case of high-rise building or towers), which are acting on the body of the structure, will transfer more smoothly to the foundation.

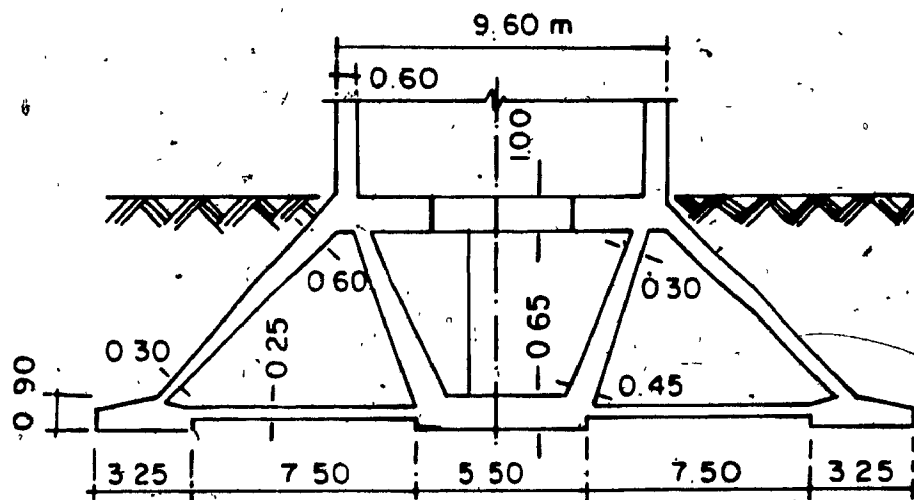


Figure 2.1 Shell Foundation of T.V. tower -Stuttgart, West Germany 1956

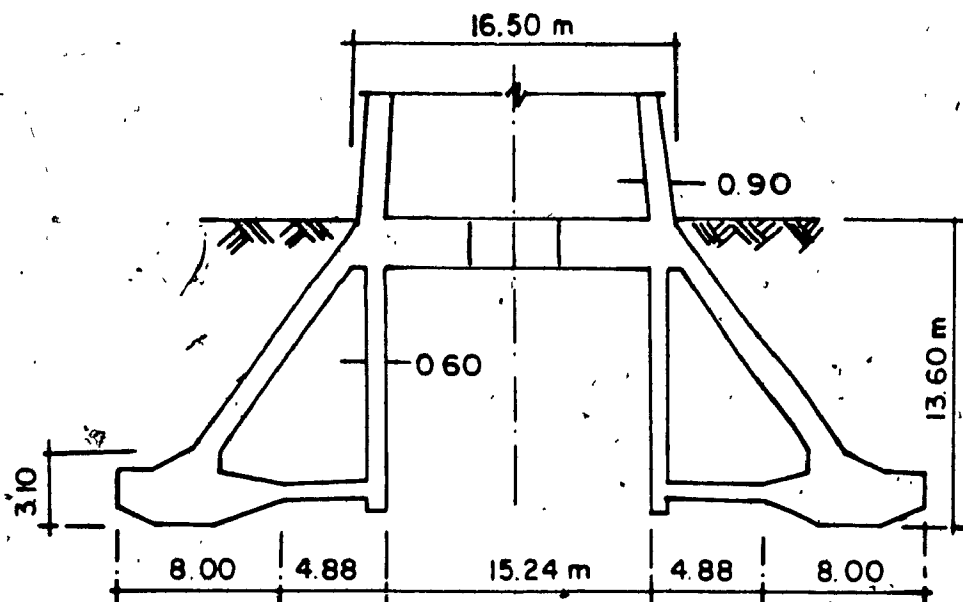


Figure 2.2 Shell Foundation of Telex tower -Hamburg, West Germany 1967

**TABLE 2-1: COMPARISON BETWEEN DIFFERENT TYPES OF FOUNDATION  
FOR DIFFERENT SOIL CONDITIONS (9):**

Project (height)	Type of Foundation	Concrete		Reinforcement		Soil Bearing Capacity(kg./cm <sup>2</sup> )
		m <sup>3</sup>	%	Ton	%	
Chimney of 45 m	Circular	146	100	8.8	100	2.5
	Empty Shell	28	19	2.5	28	
Chimney of 60 m	Circular	146	100	8.8	100	2.5
	Empty Shell	78	53	3.5	40	
Chimney of 100 m	Circular	320	100	16.0	100	2.0
	Empty Shell	107	34	6.0	38	
Chimney of 100 m	M- shell	221.5	100	23.7	100	4.0
	Empty Shell	122	55	14.6	61.5	
Chimney of 120 m	Circular	800	100	45.0	100	2.0
	Empty Shell	400	50	20.0	45	
Chimney of 150 m	Ring	966	100	68.6	100	4.0
	Empty Shell	480	50	31.5	46	

The upper cone of this foundation is usually under axial compression so the concrete can be fully utilized and therefore the construction materials can be saved.

2. Soil pressure is completely acting on the bottom of the lower cone, so the foundation level can be reduced and consequently the volume of excavation. The soil pressure produces enough amount of compression, which plays an important role to eliminate the tension force due to the horizontal force coming from the upper part, see Figure 2.3.

3. The stress distribution on the plane of intersection between the upper shell and the shear wall can be improved to avoid the local compression due to stress concentration by smoothing the surface of the upper shell and the shear wall as shown in Figure 2.4.

## 2.2 Soil Pressure Distribution

In shell foundations, the central area is always confine the soil, therefore the failure characteristics is based on contact between soil to soil giving the angle of friction equal to that of the soil material. But in case of flat footings the contact is between the base of the footing and the soil. It has been found that the friction angle between the concrete and soil/sand is varying between  $1/2$  to  $3/4$  of the value of the angle of internal friction of sand (Terzaghi et al -1967). The increase in the ultimate bearing capacity of shell foundations has been attributed to this type of soil structure interaction. It is important to determine the soil pressure distribution in both axial and radial directions for case of shell foundations, which can be explained as follows :

1. Axial forces along the lower shell (as shown in Figure 2.5): Curve I represents elastic stage at the beginning of loading. The axial strength of the lower shell is very high and the pressure distribution will be the same for both weak and strong soils. Curve II represents the soil pressure distribution, while the radial cracks are just appeared on the lower shell. The axial strength of the lower shell is reduced, soil pressure at the central

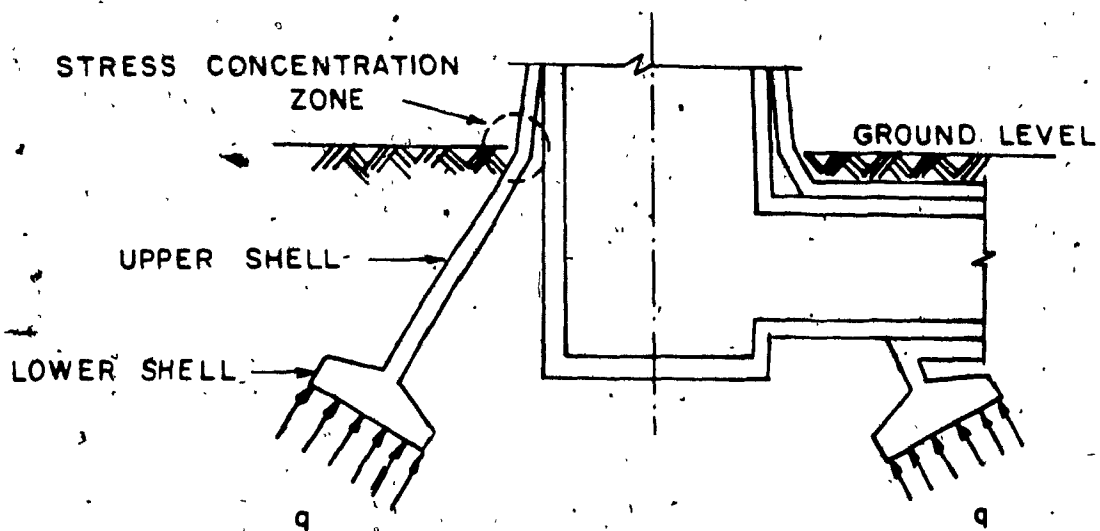


Figure 2.3 Soil Pressure Distribution on the Lower Shell

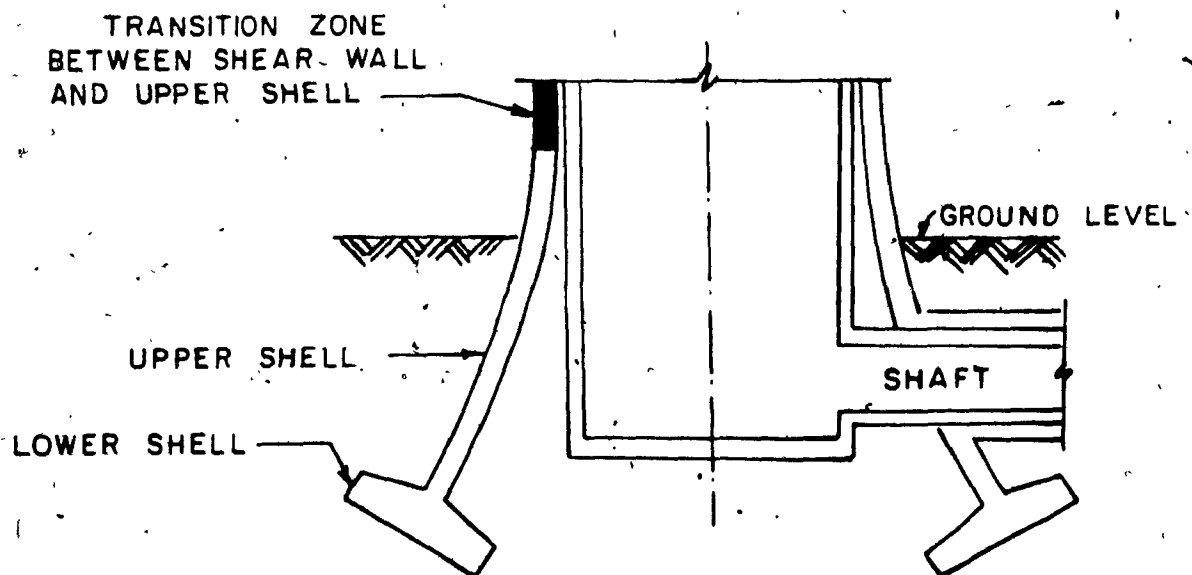
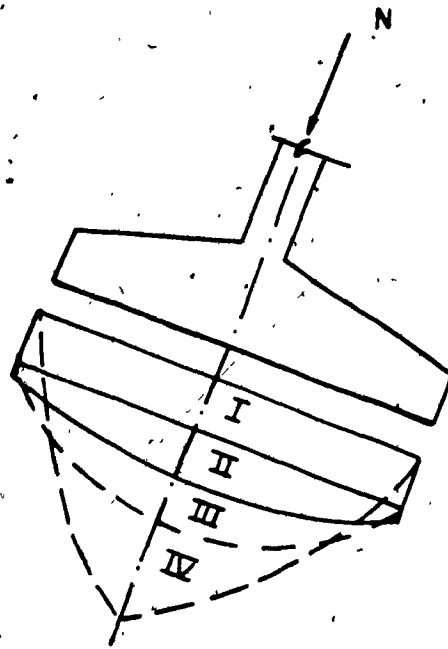
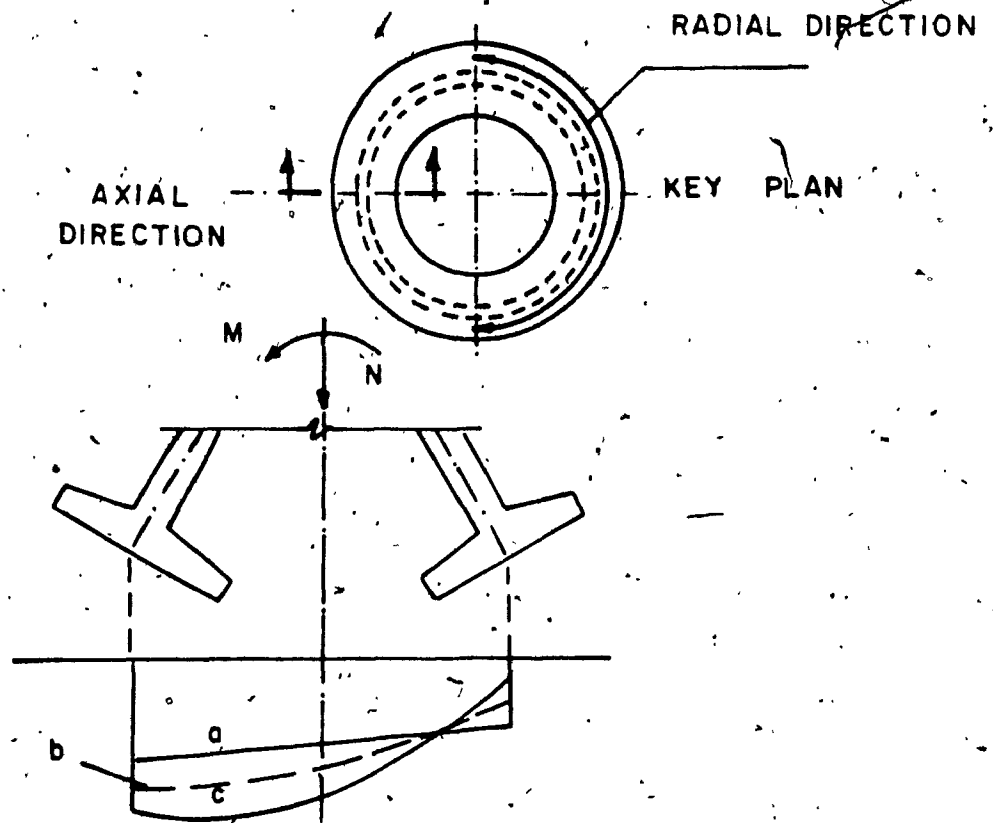


Figure 2.4 Curvature of the Upper Shell and Shear Wall



**Figure 2.5 Soil Pressure Distribution in Axial Direction**



**Figure 2.6 Soil Pressure Distribution in Radial Direction**

part increases rapidly compared to the outer perimeter where the stress increases slowly such that the resulting soil pressure distribution is no more uniform. Curve III represents the soil pressure distribution when circular cracks begin to be widen and concentration of soil pressure occurs at the center. Curve IV represents the plastic stage at which the axial strength of the lower shell is so small and the soil pressure distribution is mainly concentrated at the centre and is nearly zero at both margins (ultimate stage).

2. Radial Distribution (as shown in Figure 2.6): Because the shell foundation is a symmetric structure in space, therefore the radial forces distribute symmetrically on each cross section under central loading. Experimental data proves that because the material on each cross section of the shell is not uniformly distributed (non-homogenous), which leads to that some parts of the cross section will crack before the others. Line (a) in Figure 2.6 represents the elastic stage for the shell under eccentric load. When the shell body enters into elasto-plasto stage, the radial forces distribution is no more linearly distributed as shown in Figure 2.6 line (b). The section under maximum radial force is not increasing linearly with increasing the external force. At the ultimate stage the radial forces reach the ultimate capacity on the region subjected to the bending moment "M", while on the other side of loading, the value of the radial force is reduced.

### 2.3 Slip-line Fields and General Bearing Capacity Equation

Figure 2.7 shows a typical pattern of slip-lines in the soil beneath a foundation on the point of collapse. The regions ACD and A'C'D' are zones of passive Rankine failure. There are two families of slip-lines in these two zones inclined to each other at an angle  $(\pi/2 + \phi)$ . The regions ABC and A'B'C' are zones of radial shear, in each of which one family of slip-lines originates at the corner of the foundation (A or A'). The soil in the region ABA' may or may not be in a state of plastic failure, depending on the roughness of the underside of the foundation. If the foundation base is absolutely smooth, i.e. there



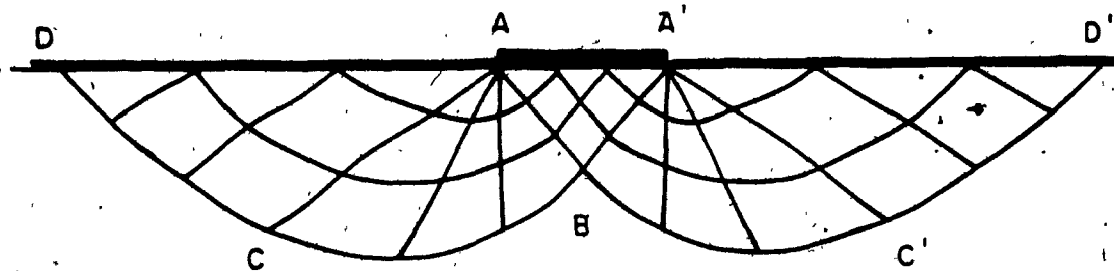


Figure 2.7 Rupture Surfaces Beneath a Foundation at Failure

is no shear stress on AA', the region ABA' is a zone of active Rankine failure. If the foundation base is absolutely rough, so that no slip takes place on AA', the zone ABA' moves downward as a rigid wedge with the foundation. The lines AB, A'B, AC and A'C' are discontinuities between the plastic zones. Any slip-line which crosses one of these lines must be continuous, but the shape of the slip-line differs on either side of the discontinuity.

By modifying a bearing capacity equation developed by Prandtl (1920) for an infinite strip, Terzaghi in (1943) was the first to present a comprehensive theory for the evaluation of ultimate bearing capacity of shallow foundation. There is some variance of opinion of how to compute the ultimate bearing capacity correctly over the past 44 years, a large number of equations/procedures have been proposed, but at present only Terzaghi equation and those subsequent by Meyerhof (1953, 1963) and later by Hansen (1970) have received enough use to say that they have survived. In the present work we will study only the case of triangular and flat strip footings (i.e. plane strain condition) resting on stiff soil (i.e. case of general shear failure) using the theory of plasticity to present a modification to the original bearing capacity equation for the case of triangular shell strip footing.

No closed solutions have been obtained for the bearing capacity of foundations on soils which have weight. If we assume that we can apply the principle of superposition, and write for the flat footing:

$$q_u = cN_c + q_0 N_q + 1/2 B\gamma N_\gamma \quad (2.1)$$

Where  $N_c$  and  $N_q$  have the values obtained for weightless soil and  $N_\gamma$  is a coefficient defining the bearing capacity of a soil having weight but no cohesion or surcharge  $c=q=0$ .

Terzaghi estimated that for  $\phi = 34^\circ$  the error in the computed value of  $q_u$  is about 10%.

Other researchers have found rather greater discrepancies in some cases, but the

procedure is sufficiently accurate for use in practice. Table 2.2 shows values of  $N_\gamma$  obtained by five different methods.

One of the most convenient and probably as accurate as any expression available for calculating  $N_\gamma$  is the one given by Hansen (1970).

$$N_\gamma = 1.8 (N_q + 1) \tan \phi \quad (2.2)$$

**TABLE 2-2: VALUES OF COEFFICIENT "N<sub>y</sub>" BY DIFFERENT METHODS (11)**

$\phi$ (Degrees)	Terzaghi	Meyerhof	Sokolovskii	Chen	Hansen
0	0.00	0.00	0.00	0.00	0.00
5	0.05	0.05	0.17	0.46	0.09
10	0.60	0.60	0.60	1.31	0.47
15	1.80	1.80	1.40	2.94	1.42
20	4.90	4.80	3.20	6.20	3.54
25	11.10	10.70	6.90	12.97	8.11
30	24.00	22.90	15.30	27.67	18.08
35	51.80	48.40	35.20	61.49	40.70
40	128.00	116.00	86.50	145.30	95.45

## CHAPTER 3

### EXPERIMENTAL INVESTIGATION

#### 3.1 General

The experimental study was carried out on five strip foundation models (i.e. plane strain condition), which have the same width and length (i.e. the horizontal projection of the bearing area is the same). The first model was flat in type (i.e. the peak angle  $\theta$  equal to  $180^\circ$ ) and the other four models had triangular shape with peak angles of  $140^\circ$ ,  $100^\circ$ ,  $90^\circ$ , and  $60^\circ$ .

The material which was used as supporting soil for the foundation models is "Morie Sand" which is imported from the U.S.A. This particular material was selected because of its homogenous quality.

Each model had been loaded twice, the first time was surface loading and the second time was buried loading with embedment ratio  $D/B=0.75$ .

The aim of this experimental investigation was to establish the effect of changing the inclination of the contact surface between foundation and soil on the ultimate bearing capacity (i.e. the effect of changing the peak angle  $\theta$  on the values of the ultimate bearing capacity coefficients  $N_q$ ,  $N_\gamma$  for the case of flat foundations).

#### 3.2 Description of the Foundation Models

The models were fabricated of stainless steel at Concordia University machine shop. In all models the base portion is of monolithic construction, with stem portion, which takes the vertical load, being fabricated separately, and then securely fastened by steel screws to the base. In all models the bearing area is covered with sand paper to give better interaction between the sand and the models. The length and the width of all models are the same, which makes the horizontal projection of their bearing area the same as well.

In each of these models three round-holes of diameter 1.0 inch evenly spaced in the longitudinal direction of the models and they were drilled down through the stem portion to allow the filling of the void areas with sand. Plugs for these holes were provided with their insertion and removal being facilitated by having them attached to a cap that fits over the top of the footing stem.

Figure 3.1 shows sketches of the five models with their dimensions to describe the physical features of each. Figure 3.2 shows end views of the five models and Figure 3.3 shows the top views of the triangular models with their caps removed to reveal the filling holes.

### 3.3 Description of the Experimental Set-up

The experimental procedure was divided into three main stages and for each stage there is a specific equipment which can be separately listed and briefly described as follows:

#### a) Sand Spreading Equipment

The equipment for the sand spreading operation consists of :

1. Overhead hopper type steel reservoir for feeding sand.
2. Vertical steel pipe with butterfly type shut-off valve leading down from the bottom of hopper to a plastic reservoir of 1. cu.ft. capacity.
3. Plastic tube extending from the bottom of the plastic reservoir for 17 inches, with copper spreading flange equipped with shut-off gate at the lower end of the plastic tube.
4. Rectangular testing tank located 26 inches below the spreading flange. The sides of this tank are made of plexiglass, while the ends are made of wood. The tank is mounted on a wheeled dolly. The inside dimensions are length = 34 in., height = 19 in., and width = 5 1/16 inches, ( Note that the width of the tank is just slightly more than the length of the models ) which can insure the plane strain condition.

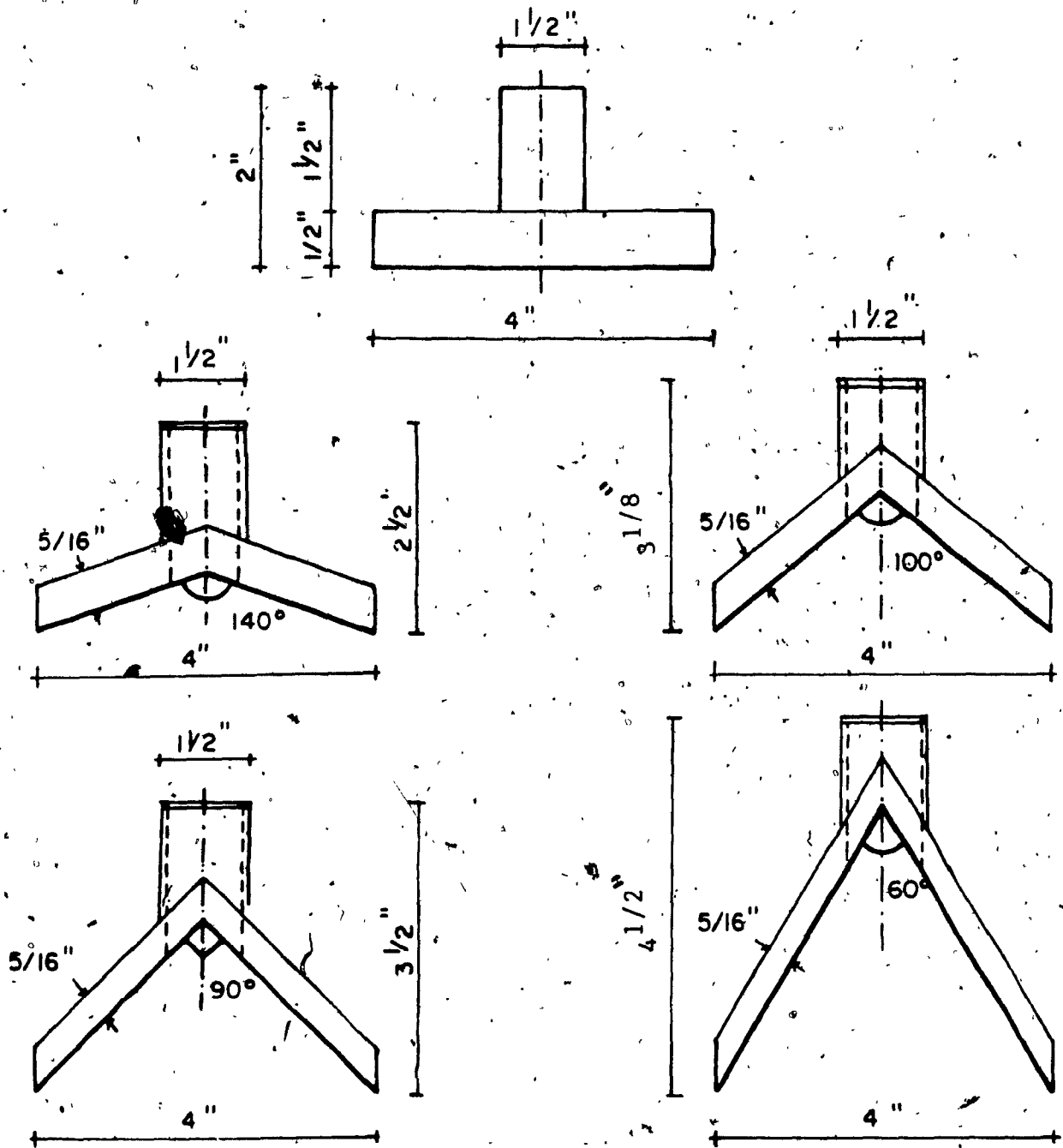
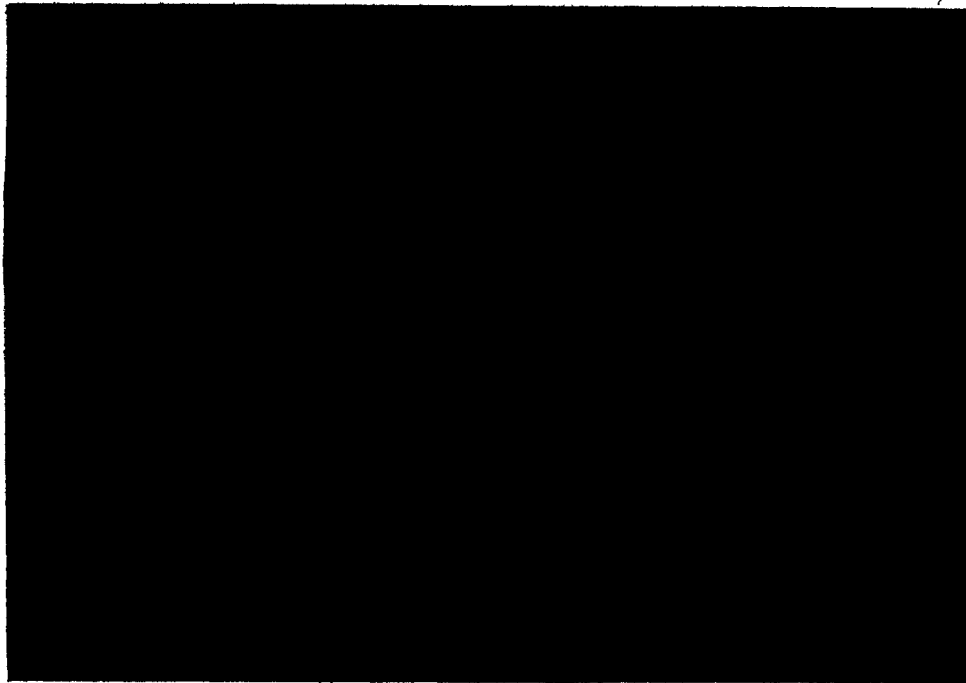
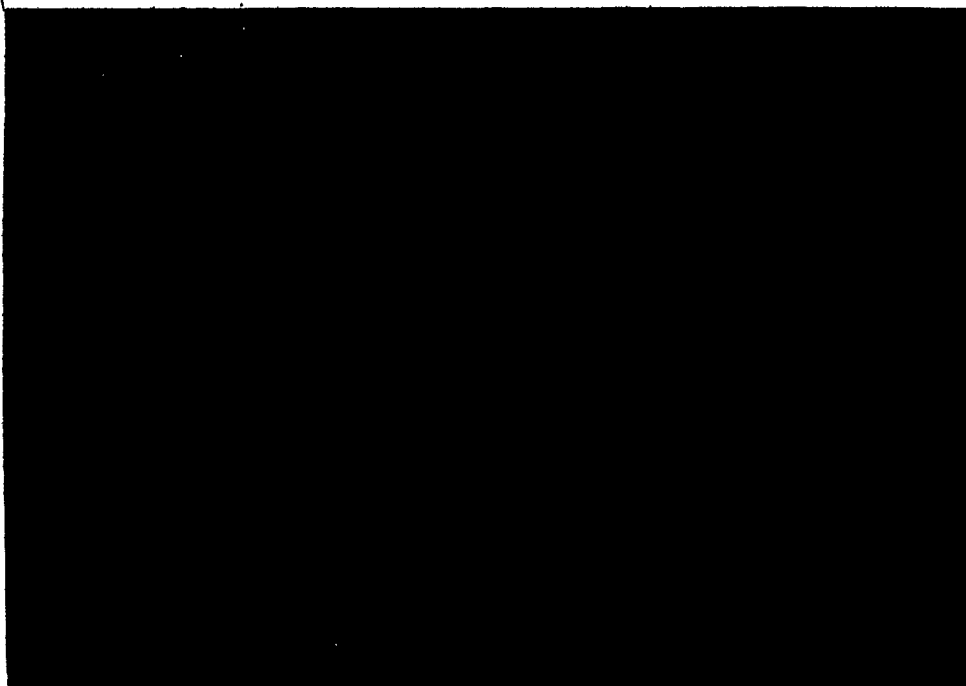


Figure 3.1 Cross Sections of the Foundation Models



**Figure 3.2 End View of the Foundation Models**



**Figure 3.3 Top View of the Triangular Models**



5. Commercial vacuum cleaner to remove the sand from the tank after testing, and to return it by flexible hose back to the overhead hopper.
6. Plastic enclosure supported in steel frame to enclose the sand spreading operation.
7. Commercial, electricity operated dust filter, used to keep the working area inside the enclosure free of dust.

Figure 3.4 shows overall view of the whole equipment used for the sand spreading operation. Figure 3.5 shows the testing tank during the spreading operation. Figure 3.6 shows the testing tank and a foundation model installed on top.

#### b) Equipment for Moving the Filled Tank

The movement of the testing tank filled with sand around the laboratory was accomplished as follows:

1. The wheeled dolly was used only to move the tank outside the sand spreading enclosure.
2. Overhead crane with lifting cables, hooks and two straps used to lift the filled tank from the wheeled dolly and place it on the platform of the compression testing machine and also to return it back on the wheeled dolly after completion of the loading operation. Figure 3.7 shows filled tank with footing model installed at top, sitting on wheeled dolly outside the sand spreading enclosure with lifted straps attached, being lifted by the overhead crane up to the platform of the compression testing machine, this showed in Figure 3.8.



**Figure 3.4 Overall view of the Sand Spreading Enclosure**

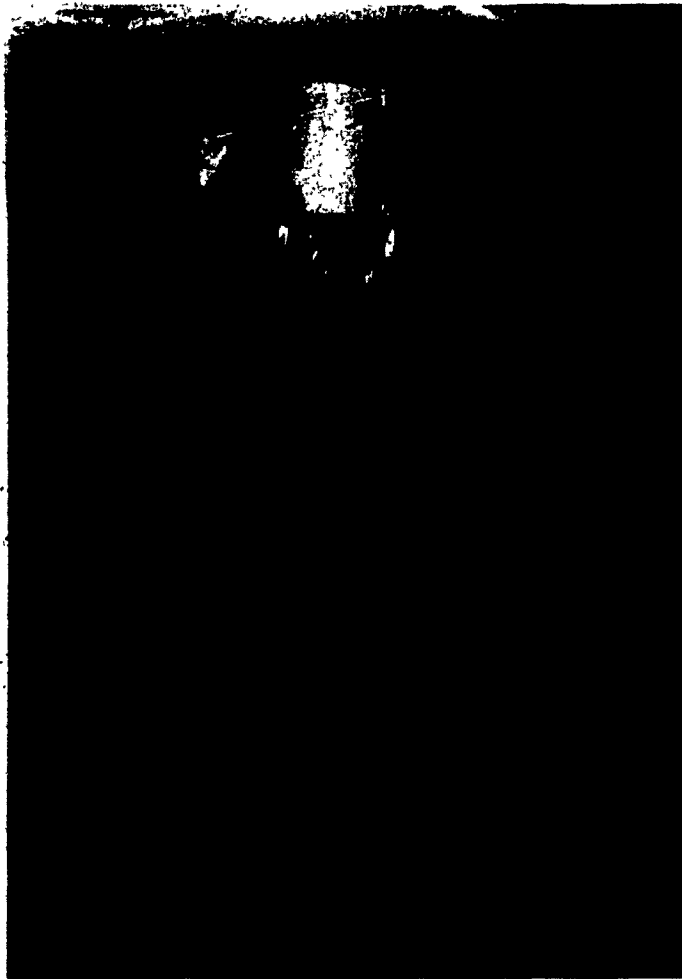


**Figure 3.5 The Testing Tank During Sand Spreading Operation**



**Figure 3.6 The Testing Tank with Foundation Model on Top**

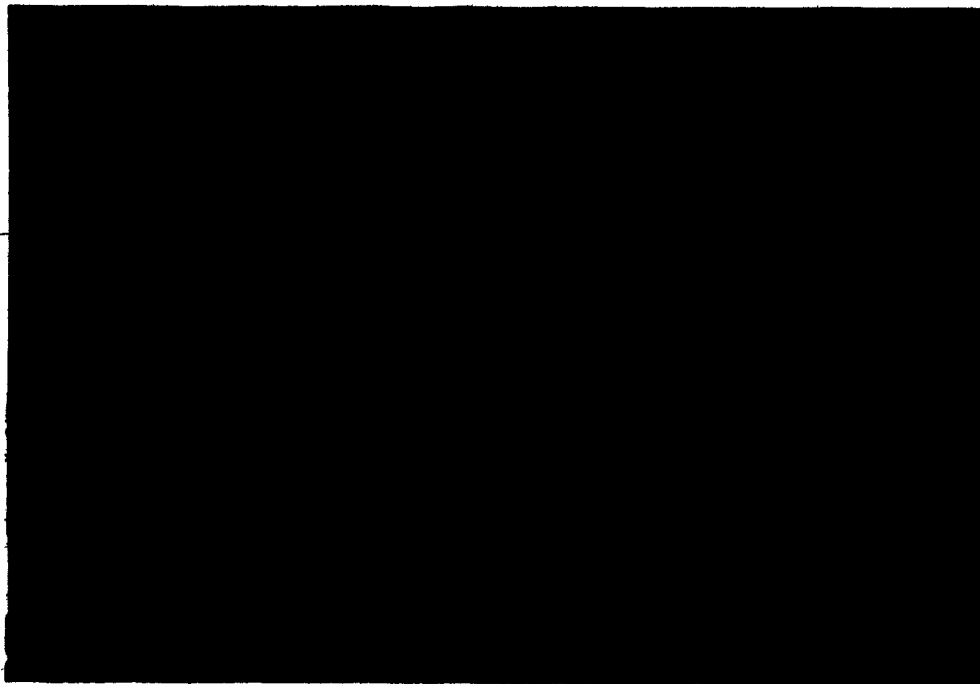


**Figure 3.7 The Testing Tank Hung up with Straps**

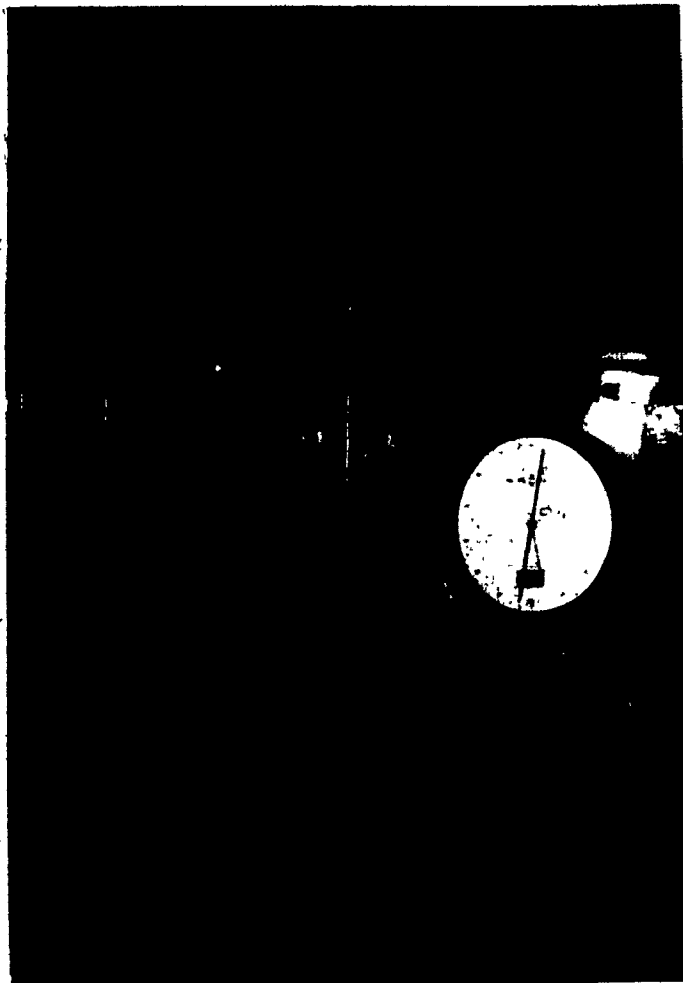


**Figure 3.8 The Testing Tank on the Platform of the Compression Machine**

### c) Load Testing Machine

The loading operation was accomplished with the following equipments:

1. Tinius Olsen compression testing machine, using hydraulic drive. Load range was set at low to give increments of 2.5 lbs.
2. A round pointed steel piston to apply the single point load to top of model footings.
3. Standard dial guage, reading in 0.001 inch graduation, to measure the settlement of the footings as the load is applied. Figure 3.9 shows general view of entire testing machine and Figure 3.10 shows close up of the tank top, as steel piston applies load to the model.

## 3.4 Experimental Procedure and Results

### 3.4.1 Soil Classification

A grain size distribution analysis was carried out on sand and the results are presented on Figure 3.11. This test together with visual inspection allow this sand to be classified as a clean, angular, cohesionless, homogenous, quartz sand and the uniformity coefficient was found to be 1.35.

The sand has an average value of specific gravity equal to 2.678. To ensure that the sand used for the loading test was compacted in a consistent and even manner, controlled spreading was employed using the technique described in previous section. This spreading technique was designed so that the minimum height of drop for sand free falling into the testing tank is 26 inches. From Figure 3.12 which shows a plot of unit weight of this particular sand versus height of drop, it can be seen that increasing the height of drop above 26 inches produces only a negligible increase in the unit weight of sand, thus the spreading system used was expected to compact the sand to essentially the same density all over the tank.

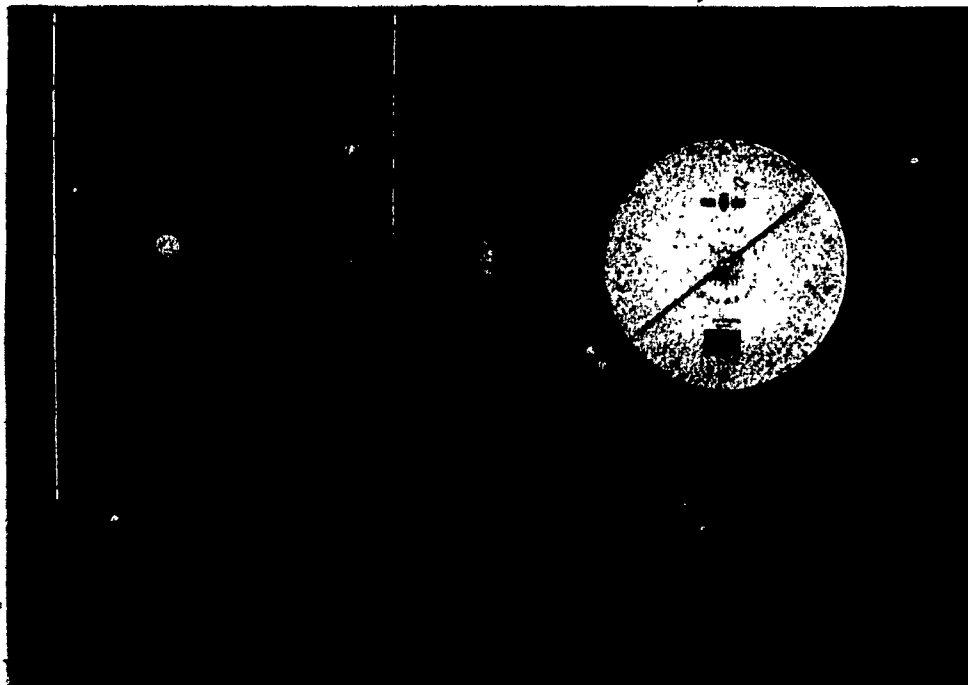


**Figure 3.9 Overall View of the Compression Machine**



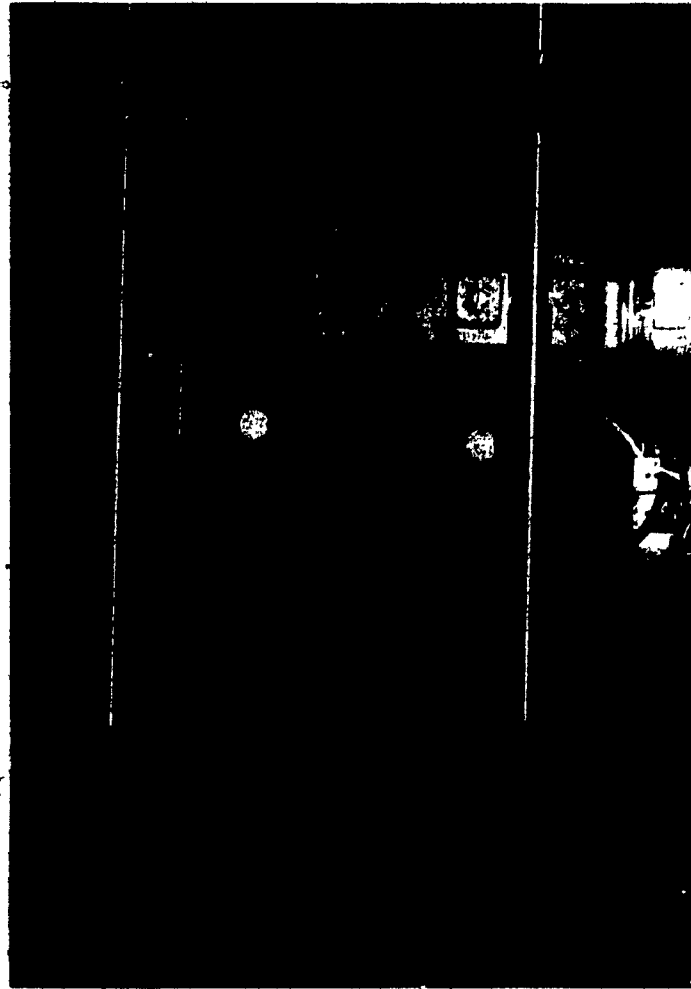


**Figure 3.10 Close-up View During Loading Test**

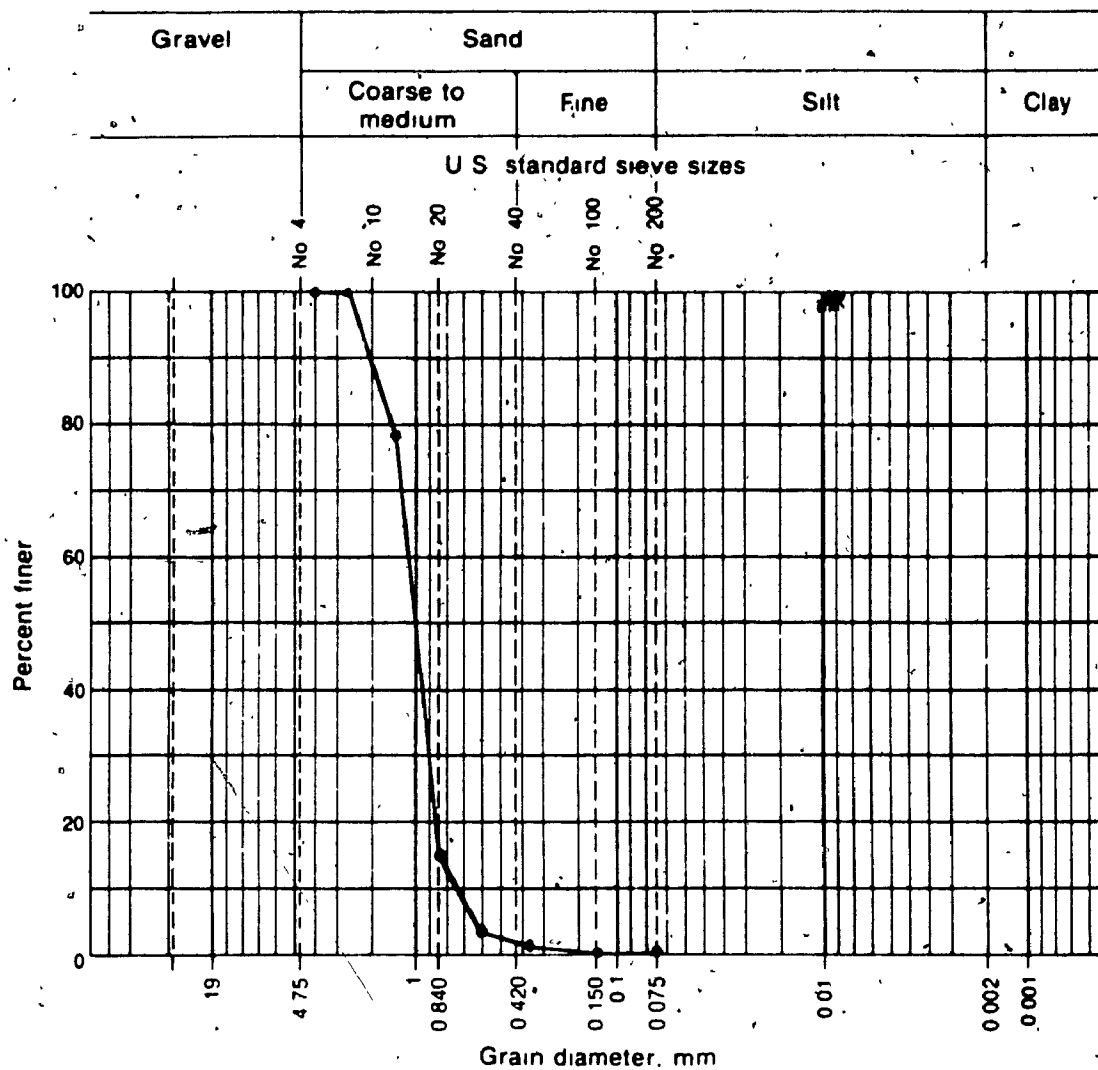


**Figure 3.11 Sieve Analysis**

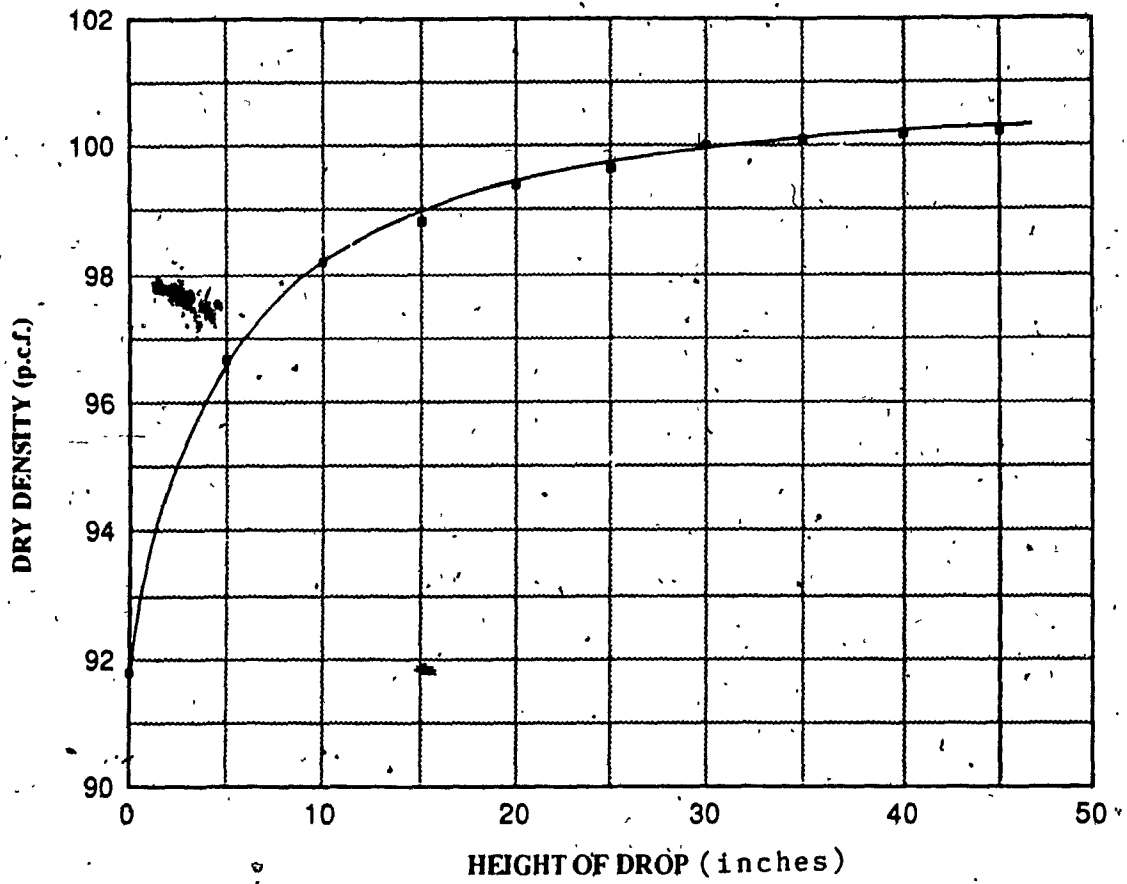


**Figure 3.12 Plot of the Unit Weight versus the Height of Drop**

The average unit weight of this sand was calculated from nine different locations within the testing tank. Three of these locations were at the bottom, the next three at level 1/3 of the tank height and the last three at 16 inches from the bottom of the tank. The unit weights were obtained by placing density cans of known weight and volume on the mentioned levels, and then filling the tank with sand using the same spreading system as used when filling for the loading test. After completing the spreading operation until the top of the tank, the same moving operation was applied to ensure that the unit weight which will be determined will be the same as the unit weight of the testing soil. Then the cans were removed, excess sand was scraped off, each can full of sand was weighted and the density of each was calculated. An average unit weight of 100.0 p.c.f was obtained. A direct shear test was conducted for a sample with the same average unit weight and the angle of internal friction ( $\phi$ ) was found to be 43 degrees. The test results are presented in Figures 3.13 and 3.14.

#### 3.4.2 Step by Step Test Procedure

The experimental procedure that was followed in order to carry out the loading test and thus establish "Load versus Settlement" relation for each model is divided into three distinct stages and these separately described as follows:

Firstly, the sand was let down from the overhead hopper through the steel pipe in order to fill the plastic reservoir. This flow was controlled with the adjustable "butterfly" shut-off valve. When the plastic reservoir became filled, the spreading operation was started by opening the shut-off gate on the spreading flange. Thus allowing sand to flow from the reservoir down through the plastic tube and out through the flange which has to be moved in steady motions by hand, back and forth over the top of the tank in the lengthwise direction. That resulted in a homogenous degree of compaction with an average

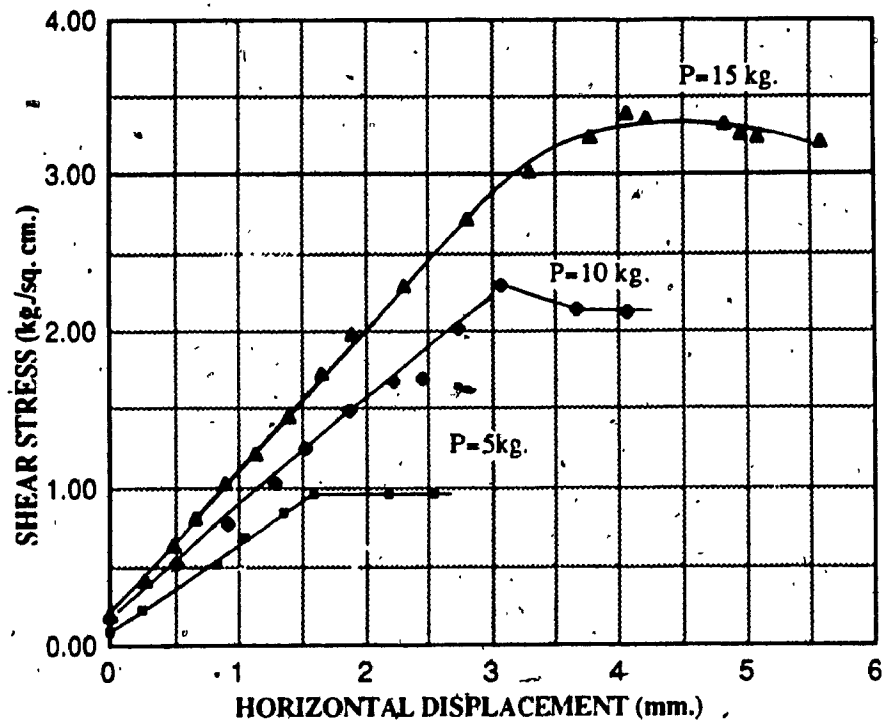


Figure 3.13 Direct Shear Test Results

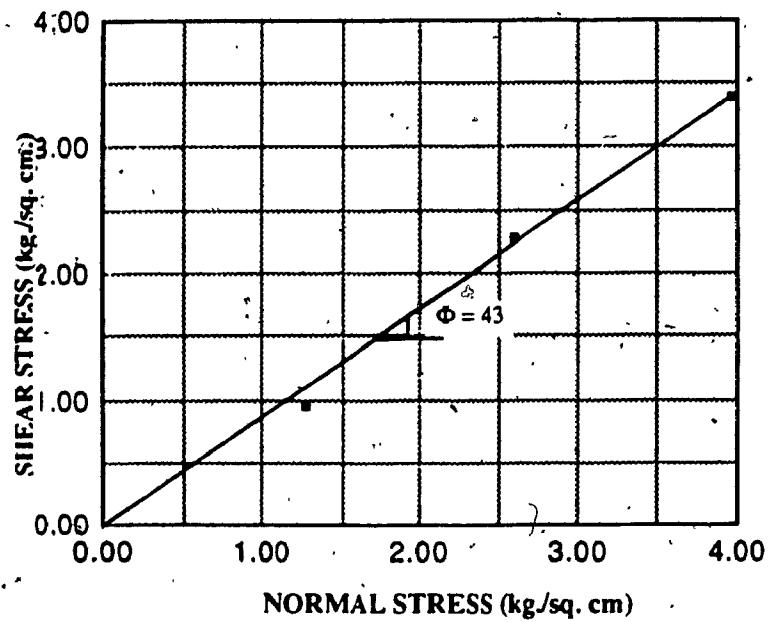


Figure 3.14 Angle of Internal Friction of Sand  $\Phi$

density of 100.0 p.c.f., and this confirms within reasonable limits the expected results from the curve of unit weight versus height of drop as presented in Figure 3.12. When the spreading operation raised the surface level of sand in the tank to where it is indicated outside the tank (level of 16 inches from the base), the spreading was stopped and then the footing was set in place lengthwise across the tank's width at the centre of the tank area, with care being taken to ensure it is seated in a level position on the sand surface. A small carpenter's level is employed for this operation.

The procedure followed here differed, however depending on whether the model is the flat or the triangular one and whether the phase loading will be on the surface of the sand or with embedded depth.

a. For the flat foundation model: once the footing was in proper position and the condition of loading will be on the surface the tank was moved to the compression machine as will be described later. If this was the buried loading condition then the spreading of sand was carried out in a continuous manner until the tank was completely full (i.e. with embedment ratio  $D/B=0.75$  ).

b. For the triangular foundation models: once the model was in proper position, its three filling holes were uncovered and utilized to hand place sand under the triangular footing until this void space was completely full. The filling holes were then again closed and the tank was moved to the compression machine. If this was the second loading condition then sand spreading was resumed until the level of sand in the tank reached a point just above the top of the footing surface. Here the spreading was stopped and the sand placed under the footing until the void space completely full. The filling holes were then again closed and the normal sand spreading operation resumed and continued, until the tank was completely full.

Secondly the tank and its contents were pushed on the wheeled dolly by hand outside the sand spreading enclosure. The overhead mounted movable crane was then used to lift the loaded tank onto the platform of the testing machine and manoeuvred by hand into the correct location underneath the load application steel piston.

With the top of the model footing now in place on the testing machine directly under the point of the load application Piston, the machine was started, then the piston began to move downwards towards the footing, until firm contact was made. At this point the machine was stopped from moving downwards, and a dial guage was set up to measure the movement of the model footing relative to the base of the compression testing machine. This movement was the total settlement of the model footing as a result of the applied vertical load. With this dial guage now set at zero the testing machine was again started, thus applying a downward force from the piston to the top of the footing, which resulted in settlement of the footing into the sand. With the testing machine set at "low range" its graduation marks were at 2.5 lbs. intervals, and as the loading and resulting settlement proceeded in a consistent and uninterrupted manner, a dial guage reading was recorded as each 25.0 lbs. increment was reached. The load application was continued until it was considered that failure have been reached, at this time the testing machine was stopped.

The results of load versus settlement are presented in tabular form in sheets 1 and 2 of Appendix A. For each test there are two columns of readings, with one showing the applied vertical load in pounds, while the other shows the corresponding downward settlement in 0.001 inches. These readings of load and corresponding settlement are plotted in Figure 3.15 and 3.16 as "load versus settlement" curves. Each Figure contains five curves, which represent a test set, i.e. a curve for each of the five footing models. For accuracy each test was repeated at least twice. At this stage it can be stated that one of the main objectives of this study have been realized, because it is clearly demonstrated

in both graphs, that the model with peak angle equal to  $60^\circ$  has the greater ultimate bearing capacity, than the other models. A further examination of the "load versus settlement" curves shows that the settlement characteristics are consistent through all ranges of loading and under the same vertical loading condition a footing of the flat conventional type will allow the most settlement, while a footing of peak angle equal to  $60^\circ$  will settle by the least amount. The point of general shear failure or ultimate bearing capacity is often not very well defined. A very versatile ultimate load criterion that can recommended for general use defines the ultimate load as the point where the slope of the load-settlement curve first reaches zero or a steady minimum value (Vesic, 1963). Another consistent ultimate load criterion, suggested in recent years by Christiaens (DeBeer, 1967), defines the ultimate load at the point of break of the load-settlement curve in a log/log plot. From the curves generated from the laboratory tests results which are shown in Figures 3.15 and 3.16 and by applying Vesic concept we can define the ultimate load for each model as presented in Table 3.1 and the value of the ultimate load for each model is showed with vertical broken line in both figures.



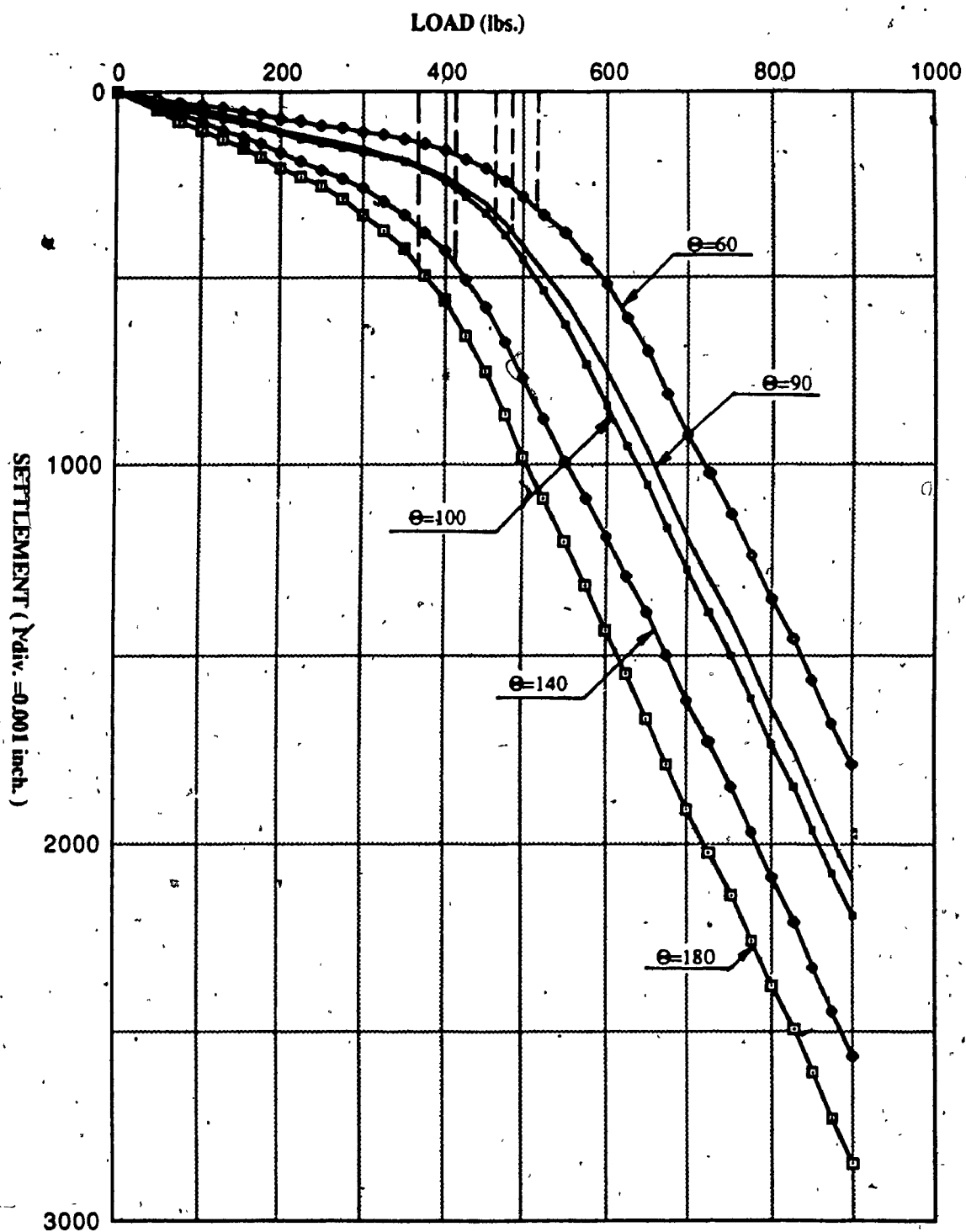


Figure 3.15 Load versus Settlement - Surface Loading

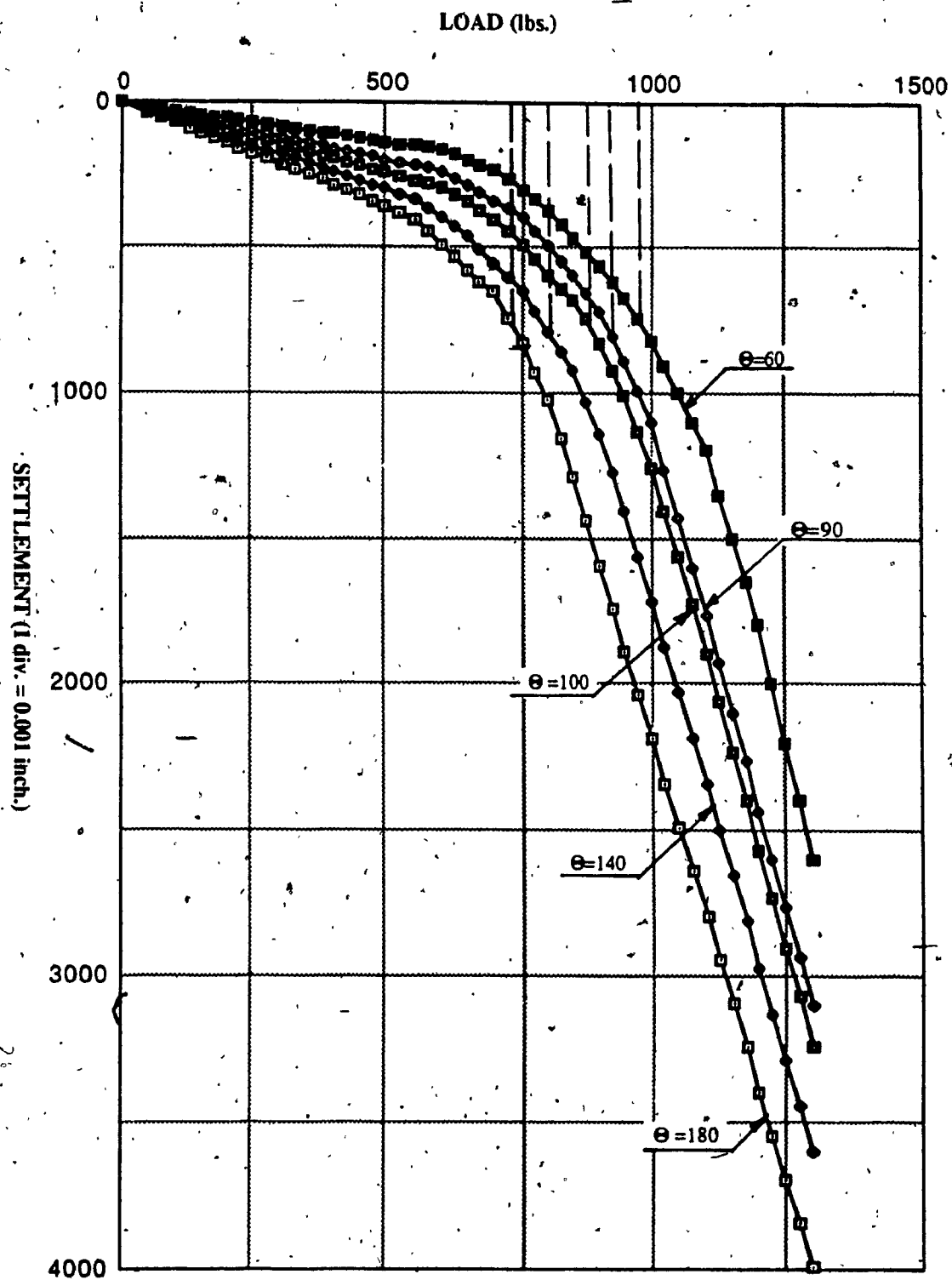


Figure 3.16 Load versus Settlement -Buried Loading( $D/B=0.75$ )

**TABLE 3.1: ULTIMATE BEARING CAPACITY FOR THE FOUNDATION  
MODELS:**

Peak Angle ( $\theta$ )	Ultimate Load (lbs.)	
	surface loading	buried loading
180	370	720
140	410	800
100	460	890
90	480	920
60	520	990

## CHAPTER 4

### ANALYSIS OF THE THEORITICAL MODEL.

#### 4.1 General

The foundation with which we are concerned in this study is strip footing. The longitudinal strain in and under such footing can only be negligible, and no serious error is introduced by assuming the condition of plane strain. In this chapter, the collapse load is only derived for the plane strain state, but the principles adduced apply equally to analysis of collapse in three dimensions.

Real soils commonly have stress-strain curves of the type shown by the solid line in Figure 4.1. With increasing shear strain, the shearing resistance increases to a peak value and then drops to a nearly constant residual values, between these values the material is said to work soften.

The method of analysis of our model assumes that the yield condition is independent of strain, so that the stress-strain curve is of the form shown by the broken line in Figure 4.1. A material with this form of yield condition is said to be perfectly plastic. Yield and failure conditions in this case are identical.

If the predicted collapse load is to be reliable, it is important that the average resistance of the real soil should match that of the model soil within the plastic zone. Clearly, if the strain in the real soil is nearly uniform at the collapse load, much of this soil will develop its peak resistance at the same moment. The greatest average resistance will be near the peak value. In some structures, however, much of the soil undergoes substantial plastic strain before collapse. In such cases, the average resistance in the plastic zone is much nearer to the residual value. Some care is therefore needed in choosing the values to be assigned to parameters defining the failure condition of the model soil. These values will depend on the collapse mechanism of the structure, as well

as on the properties of the real soil.

When a structure formed of perfectly plastic materials is on the point of collapse, a zone of material must exist which has reached the limit of its shear strength. This zone must be sufficiently extensive to form an unstable mechanism. Within this plastic zone, stress and strain components must satisfy the following :

(a) The Condition of Equilibrium in Plane Strain

If we consider a body, in Figure 4.2, in which the stress components vary with X and Z, and in which there are body forces X and Z per unit volume of the material, acting in the X and Z directions respectively.

Each element within the body must be in equilibrium under the effect of the stresses on the boundaries of the element and of the body forces acting within it. For the case of plane strain in the X-Z plane, this condition is satisfied if:

- (1) there is no moment about an axis normal to the X-Z plane
- (2) there is no resultant force on the element in either of the X or Z directions

The first of these conditions requires that :

$$\tau_{xz} = \tau_{zx} \quad (4.1)$$

The second condition shows that :

$$(\delta\sigma_x / \delta x \, dx) \, dydz + (\delta\tau_{xz} / \delta z \, dz) \, dxdy + X \, dxdydz = 0 \quad (4.2)$$

$$(\delta\sigma_z / \delta z \, dz) \, dxdy + (\delta\tau_{xz} / \delta x \, dx) \, dydz + Z \, dxdydz = 0 \quad (4.3)$$

$$\delta\sigma_x / \delta x + \delta\tau_{xz} / \delta z + X = 0 \quad (4.4)$$

$$\delta\sigma_z / \delta z + \delta\tau_{xz} / \delta x + Z = 0 \quad (4.5)$$

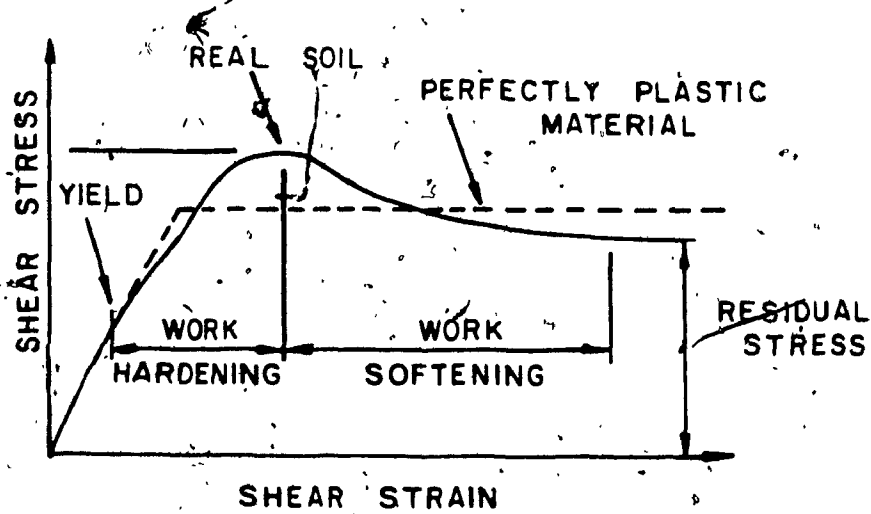


Figure 4.1 Stress/Strain Relationships

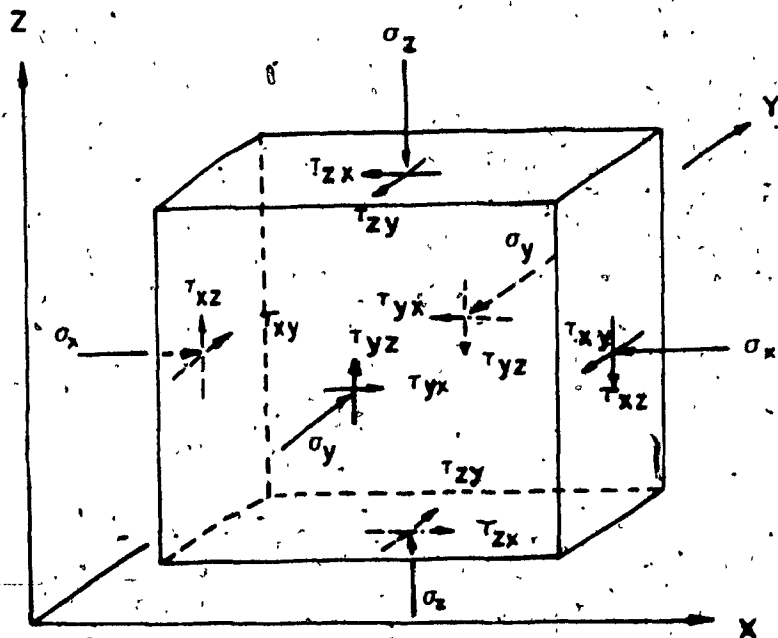


Figure 4.2 Stress Components in Cartesian Coordinates

If the weight of the material is the only body force, and if the x-axis is inclined with an angle  $\xi$  to the horizontal, we can define the equilibrium condition in terms of total stress as follows :

$$\delta\sigma_x / \delta x + \delta\tau_{xz} / \delta z + \gamma \sin \xi = 0 \quad (4.6)$$

$$\delta\sigma_z / \delta z + \delta\tau_{xz} / \delta x + \gamma \cos \xi = 0 \quad (4.7)$$

#### (b) The Yield Condition and the Flow Rule

For any perfectly plastic soil model the yield and failure conditions are identical.

The yield (and failure) condition may be stated in terms of total stress as :

$$\tau_f = c + \sigma_n \tan \phi \quad (4.8)$$

or in terms of effective stress as follows :

$$\tau_f = c' + (\sigma_n - u) \tan \phi' \quad (4.9)$$

A consequence of our assumption of perfect plasticity is that any stress state satisfying the yield condition will, if maintained, cause unlimited plastic strain. There is, therefore, no direct relationship between yield stress and plastic strain. We need to define, not the strain, but the strain rate, i.e. the rate at which the strain is increasing with respect to time. The absolute value of the strain rate is not determinate, since, in designing the soil models, we have not specified any property which could control it. It turns out to be not very important as we are concerned only with relative magnitudes of the strain rate components. These define the directions of the strain rate vectors, and the shape of the deformed body.

Knowing the strains everywhere within a body, we may determine the relative displacements of different points within it. In a similar way, knowing the strain rates, we may determine the velocities, i.e., the rates of displacements. As in the case of the strain rates, the absolute magnitudes of the velocity are not determinate. Our concern is with the relative magnitudes of the velocity components, since these define the directions of the velocity vectors and hence the directions of motion. A pattern of velocity vectors, defining the motion everywhere within the plastic zone is called a velocity field.

### (c) The Flow Rule and The Plastic Potential

In a linearly elastic body Hooke's law defines the relation between the components of stress and strain. Similarly, in a perfectly plastic body, the flow rule defines the relation between the components of the yield stress ( $\sigma_n, \tau_f$ ) and the corresponding plastic strain rates ( $\dot{\epsilon}_n^P, \dot{\gamma}^P$ ). Von Mises suggested that the flow rule might be expressed in terms of a plastic potential function ( $f$ ) which may be defined, for a Mohr-Coulomb material, by the equation :

$$\dot{\gamma}^P / \dot{\epsilon}_n^P = (\delta f / \delta \tau) / (\delta f / \delta \sigma_n) \quad (4.10)$$

Von Mises also suggested that it may often be useful to assume that the potential function is identical with the yield condition. For a Mohr-Coulomb material, where yield and failure conditions are identical for all stress states on the yield locus,  $\tau = \tau_f$  and  $f = 0$ . A flow rule defined in this way by the yield condition is said to be associated if :

$$f = \tau - c - \sigma_n \tan \phi \leq 0 \quad (4.11)$$



#### 4.2 Upper Bound Solution for Triangular Rough Strip Foundation on Weightless Soil:

In theory, the equilibrium, yield condition and the flow rule, are sufficient to determine the velocity field, stress distribution and collapse load. In practise, however, it is seldom possible to obtain a closed solution, except in very simple cases. In other cases, it is possible to obtain useful approximate solution by means of the upper bound limit theorem.

Now suppose that we choose an arbitrary velocity field, i.e. an arbitrary pattern of velocities defining the motion everywhere within soil media. If the motion is everywhere compatible with the continuity of the motion at the boundary, the velocity field is said to be kinematically admissible.

If the work done by the displacement of the load exceeds the energy dissipated in deforming the body, the velocity field is said to be unstable. For a perfectly plastic material with an associated flow rule, it can be shown that, if any unstable kinematically admissible velocity field can be found, collapse must occur under the given load or under some smaller load. This, for any kinematically admissible velocity field, the load computed by equating the internal energy dissipation to the external work done is an upper bound to the true collapse load.

Let us consider a foundation in Figure 4.3 of width  $B$  and infinite length resting on the surface of a weightless frictional soil. The velocity field is assumed to consist of two zones of radial shear bounded by logarithmic spirals, which move between triangular rigid zones sliding on thin deforming layer.

From the geometry of Figure 4.3, the following equations can be derived:

$$JL = (B/2) \sec (\pi/4 + \phi/2 + \beta) \quad (4.12)$$

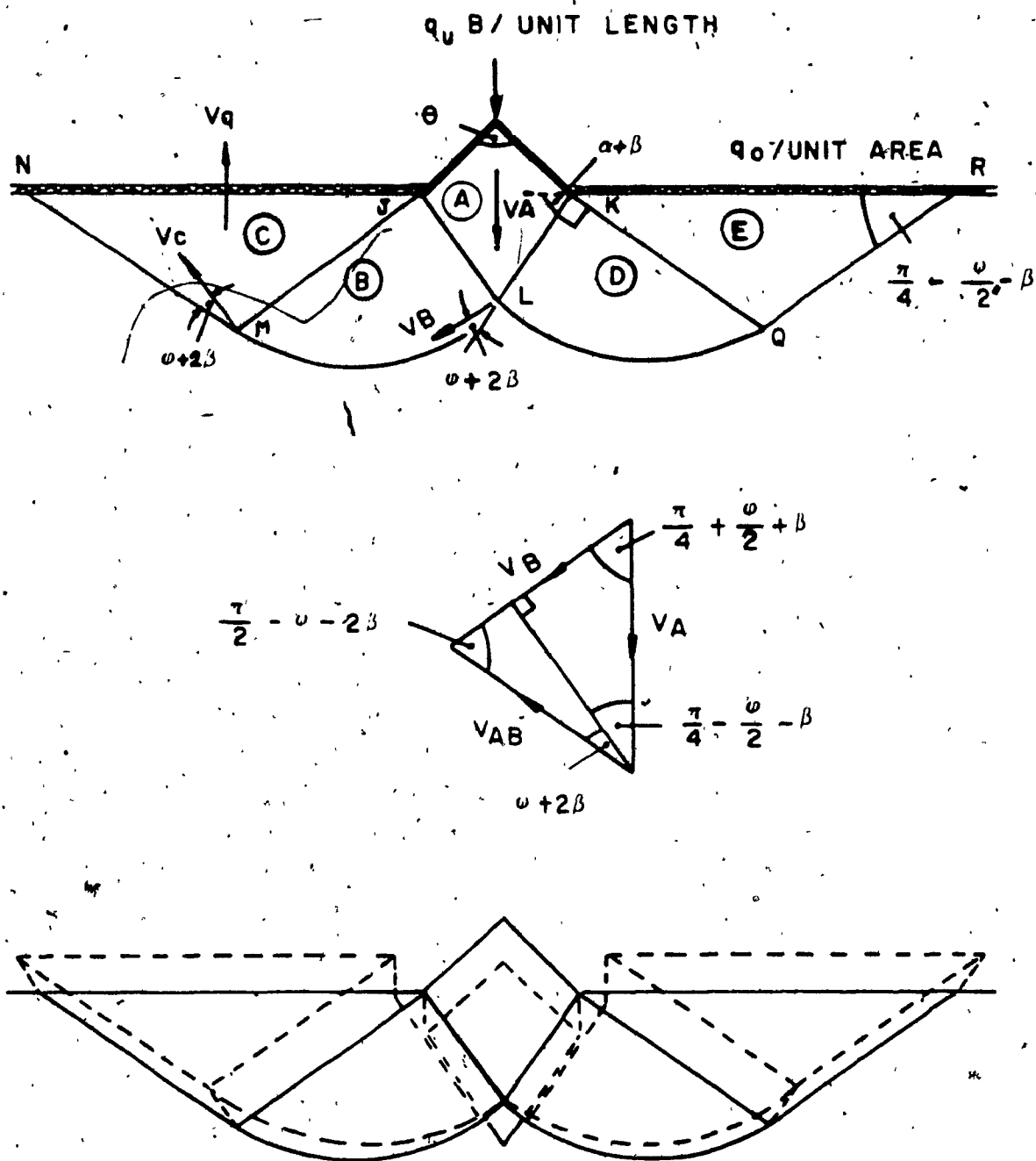


Figure 4.3 A Triangular Rough Foundation on Weightless Soil (Upper Bound Analysis)

$$JM = MN = (B/2) \exp(\pi/2 \tan(\phi + 2\beta)) \sec(\pi/4 + \phi/2 + \beta) \quad (4.13)$$

$$JN = 2 (B/2) \exp(\pi/2 \tan(\phi + 2\beta)) \sec(\pi/4 + \phi/2 + \beta) \cdot$$

$$\sin(\pi/4 + \phi/2 + \beta)$$

$$= B \exp(\pi/2 \tan(\phi + 2\beta)) \tan(\pi/4 + \phi/2 + \beta) \quad (4.14)$$

Where angel  $\beta$  assumed to be equal to  $1/120 (\pi - \theta)$ .

Let zone A move down with velocity  $V_A$ . The direction of motion of zone B at L must be inclined at  $(\phi + 2\beta)$  to the logarithmic spiral LM and normal to JL. From the velocity diagram (Figure 4.3) it may be seen that  $V_B$  (the velocity of B at L) is

$1/2 V_A \sec(\pi/4 + \phi/2 + \beta)$  while  $V_{AB}$  (the velocity of B relative to A) is

$1/2 V_A \sec(\pi/4 + \phi/2 + \beta)$  inclined at  $(\phi + 2\beta)$  to JL. Zone C moves with

$$\text{velocity: } V_C = 1/2 V_A \exp(\pi/2 \tan(\phi + 2\beta)) \sec(\pi/4 + \phi/2 + \beta) \quad (4.15)$$

and inclined with angle  $(\phi + 2\beta)$  to MN, and the ground surface JN rises with a

$$\text{velocity: } V_q = V_C \sin(\pi/4 + \phi/2 + \beta)$$

$$= 1/2 V_A \exp(\pi/2 \tan(\phi + 2\beta)) \tan(\pi/4 + \phi/2 + \beta) \quad (4.16)$$

The rate of the external work is given by the following equation:

$$q_u B V_A - 2q_0 (B V_A / 2) (\exp(\pi/2 \tan(\phi + 2\beta)) \tan(\pi/4 + \phi/2 + \beta))^2$$

$$= B V_A (q_u - q_0 \exp(\pi \tan(\phi + 2\beta)) \tan^2(\pi/4 + \phi/2 + \beta)) \quad (4.17)$$

The rate of dissipation of energy on JL, KL, MN and QR is given by :

$$\begin{aligned} & \Sigma c l v \cos (\phi + 2 \beta) \\ & = 2 c(B/2)(V_A/2) \sec^2 (\pi / 4 + \phi / 2 + \beta) (1 + \exp (\pi \tan (\phi + 2 \beta))) \\ & \quad * \cos (\phi + 2 \beta) \end{aligned} \quad (4.18)$$

The dissipation rate in zone B and D can be determined as :

$$\begin{aligned} & \Sigma c r V \cot (\phi + 2 \beta) (\exp (\pi \tan (\phi + 2 \beta)) - 1) \\ & 2 c (B/2)(V_A/2) \sec^2 (\pi / 4 + \phi / 2 + \beta) (\exp (\pi \tan (\phi + 2 \beta)) - 1) \cot (\phi + 2 \beta) \end{aligned} \quad (4.19)$$

By collecting terms and noting that :

$$\sec^2 (\pi / 4 + \phi / 2 + \beta) = 2 / (1 - \sin (\phi + 2 \beta)) \quad (4.20)$$

The total dissipation rate is :

$$\begin{aligned} & c B V_A \cot (\phi + 2 \beta) (1 / (1 - \sin (\phi + 2 \beta))) (\sin (\phi + 2 \beta) \\ & \quad * (1 + \exp (\pi \tan (\phi + 2 \beta))) + \exp (\pi \tan (\phi + 2 \beta)) - 1) \\ & = c B v_A \cot (\phi + 2 \beta) (\exp (\pi \tan (\phi + 2 \beta)) \tan^2 (\pi / 4 + \phi / 2 + \beta) - 1) \end{aligned} \quad (4.21)$$

Equating the external work done to internal energy dissipated (4.17&4.21) we get:

$$q_u = c N_{ct} + q_o N_{qt} \quad (4.22)$$

$$\text{Where: } N_{qt} = \exp (\pi \tan (\phi + 2 \beta)) \tan^2 (\pi / 4 + \phi / 2 + \beta) \quad (4.23)$$

$$N_{ct} = \cot(\phi + 2\beta)(N_{qt} - 1) \quad (4.24)$$

and knowing the factors  $N_q$ ,  $N_c$  for flat footing are :

$$N_q = \exp(\pi \tan \phi) \tan^2(\pi/4 + \phi/2) \quad (4.25)$$

$$N_c = \cot \phi (N_q - 1) \quad (4.26)$$

then we can define the new coefficients for triangular shell strip footings as :

$$\begin{aligned} N_{qt} &= \exp(\pi(\tan \phi + \tan 2\beta) / (1 - \tan \phi \tan 2\beta)) \\ &\quad * ((\tan(\pi/4 + \phi/2) + \tan \beta) / (1 - \tan(\pi/4 + \phi/2) \tan \beta))^2 \\ &= \exp(\pi(\tan \phi - \tan \phi + ((\tan \phi + \tan 2\beta) / (1 - \tan \phi \tan 2\beta)))) \\ &\quad * \tan^2(\pi/4 + \phi/2) / \tan^2(\pi/4 + \phi/2) \\ &\quad * ((\tan(\pi/4 + \phi/2) + \tan \beta) / (1 - \tan(\pi/4 + \phi/2) \tan \beta))^2 \\ &= \exp(\pi \tan \phi) \exp(\pi(((\tan \phi + \tan 2\beta) / (1 - \tan \phi \tan 2\beta)) - \tan \phi)) \\ &\quad * \tan^2(\pi/4 + \phi/2) ((\tan(\pi/4 + \phi/2) + \tan \beta) / (\tan(\pi/4 + \phi/2) \\ &\quad - \tan^2(\pi/4 + \phi/2) \tan \beta))^2 \\ &= \exp(\pi \tan \phi) \tan^2(\pi/4 + \phi/2) \\ &\quad * \exp(\pi((\tan \phi + \tan 2\beta - \tan \phi + \tan^2 \phi \tan 2\beta) / (1 - \tan \phi \tan 2\beta))) \\ &\quad * ((\tan(\pi/4 + \phi/2) + \tan \beta) / (\tan(\pi/4 + \phi/2) - \tan^2(\pi/4 + \phi/2) \tan \beta))^2 \end{aligned}$$

substituting for  $N_q$  from equation (4.25) we can get :

$$= N_q \exp \left( \pi \left( \frac{\tan 2\beta + \tan^2 \phi \tan 2\beta}{1 - \tan \phi \tan 2\beta} \right) \right) \\ * \left( \frac{\tan (\pi/4 + \phi/2) + \tan \beta}{\tan (\pi/4 + \phi/2) - \tan^2 (\pi/4 + \phi/2) \tan \beta} \right)^2 \quad (4.27)$$

and by putting :

$$F_q = \exp \left( \pi \left( \frac{\tan 2\beta + \tan^2 \phi \tan 2\beta}{1 - \tan \phi \tan 2\beta} \right) \right) \\ * \left( \frac{\tan (\pi/4 + \phi/2) + \tan \beta}{\tan (\pi/4 + \phi/2) - \tan^2 (\pi/4 + \phi/2) \tan \beta} \right)^2 \quad (4.28)$$

we get :

$$N_{qt} = N_q * F_q \quad (4.29)$$

Similar procedure can be applied for factor  $N_c$  :

$$\cot (\phi + 2\beta) = \left( \frac{1 - \tan \phi \tan 2\beta}{\tan \phi + \tan 2\beta} \right) \cot \phi \tan \phi \\ = \left( \frac{\tan \phi - \tan^2 \phi \tan 2\beta}{\tan \phi + \tan 2\beta} \right) \cot^2 \phi \quad (4.30)$$

therefore:

$$N_{ct} = F_c \cot \phi (N_{qt} - 1) \quad (4.31)$$

$$F_c = \left( \frac{\tan \phi - \tan^2 \phi \tan 2\beta}{\tan \phi + \tan 2\beta} \right) \quad (4.32)$$

Where  $F_c$ ,  $F_q$  are factors obtained from Figures 4.4 and 4.5 respectively, which are function of the the Peak angle " $\theta$ " and angle of internal friction of the soil " $\phi$ ". For the case of flat footing  $\theta = 180^\circ$  we can find  $\beta = 0.0$  and  $F_c = F_q = 1$ .

#### 4.3 Bearing Capacity of triangular Footing on Soil Having Weight

We can apply the principle of superposition for triangular strip footing and by using Hansen expression for  $N_\gamma$  (case of flat footing) we can get the following formular:

$$q_u = c N_{ct} + q_o N_{qt} + 1/2 \gamma B N_{\gamma t} \quad (4.33)$$

Where:

$$N_{ct} = \cot \phi (F_q N_q - 1) F_c \quad (4.34)$$

$$N_{qt} = N_q * F_q \quad (4.35)$$

$$N_{\gamma t} = 1.80 (F_q N_q - 1) \tan \phi \quad (4.36)$$

The following computer program was developed to calculate these factors. The factors  $N_{ct}$ ,  $N_{qt}$  and  $N_{\gamma t}$  can be obtained from Figures 4.6, 4.7 and 4.8 respectively, which are function of the Peak angle " $\theta$ " and angle of internal friction of the sand " $\phi$ ". The angle " $\beta$ " was assumed to be zero for the case of flat footings and one degree for the case of traingular footing of peak angle 60 degrees.

```

C*****
C* THIS PROGRAM IS TO CALCULATE NEW FACTORS FOR THE BEARING *
C* CAPACITY EQUATION IN CASE OF TRIANGULAR STRIP FOOTING *
C* RESTING ON FRICTIONAL SOIL *
C*****

```

```

PROGRAM FINAL
INTEGER FI,CI
REAL NQ,NQT,NCT,NGT
OPEN (5,FILE='RESULT.DAT',STATUS='NEW')
WRITE (*,1)
1 FORMAT (/5X,' PLEASE ENTER PI')
READ (*,*) PI
WRITE (5,2)
2 FORMAT (/30X,'CONCORDIA UNIVERSITY')
WRITE (5,3) PI
3 FORMAT (//3X,'PI = ',F7.5)
WRITE (5,4)
4 FORMAT (///3X,'FI',5X,'CI',8X,'NQ',5X,'FQ',6X,'FC',8X
& 'NCT',8X,'NQT',9X,'NGT')

```

```

C*****
C* FI : THE ANGLE OF INTERNAL FRICTION OF THE SAND *
C* CI : THE PEAK ANGLE OF THE FOUNDATION *
C* NQ : ORIGINAL FACTOR OF TERZAGHI FOR BEARING CAPACITY EQN. *
C* FQ : FACTOR FOR CHANGING "NQ" *
C* FC : FACTOR FOR CHANGING "NC" *
C* NCT: NEW FACTOR FOR CASE OF TRIANGULAR FOOTING "COHESIVE" *
C* NQT: NEW FACTOR FOR CASE OF TRIANGULAR FOOTING "SURCHARGE" *
C* NGT: NEW FACTOR FOR CASE OF TRIANGULAR FOOTING "FRICTIONAL" *
C*****

```

```

DO 10 FI = 25,50,5
DO 20 CI = 60,180,20
X = 120
F = (FI*PI)/180

```



$$C = (CI \cdot \pi) / 180$$

C\*\*\*\*\*

C\* A : THE ORIGINAL FAILURE ANGLE FOR FLAT STRIP FOOTING \*

C\* B : THE INCREASE IN ANGLE "A" FOR TRIANGULAR STRIP FOOTING \*

C\* WITH MAX. VALUE OF ONE DEGREE FOR THE PEAK ANGLE OF 60° \*

C\*\*\*\*\*

$$A = \pi/4 + F/2$$

$$B = (\pi - C)/X$$

$$F1 = \exp(\pi * ((\tan(2*B) + (\tan(F))^{**2} * \tan(2*B)) / (1 - \tan(F) * \tan(2*B))))$$

$$F2 = ((\tan(A) + \tan(B)) / (\tan(A) - (\tan(A))^{**2} * \tan(B)))^{**2}$$

$$FQ = F1 * F2$$

$$FC = (\tan(F) - (\tan(F))^{**2} * \tan(2*B)) / (\tan(F) + \tan(2*B))$$

$$NQ = \exp(\pi * \tan(F)) * (\tan(\pi/4 + F/2))^{**2}$$

$$NQT = FQ * NQ$$

$$NCT = FC * (NQT - 1) / \tan(F)$$

$$NGT = 1.80 * (NQT - 1) * \tan(F)$$

WRITE (5,5) FI,CI,NQ,FQ,FC,NCT,NQT,NGT

5 FORMAT (3X,I5,2X,I5,2X,F9.3,2X,F5.3,2X,F5.3,2X,F9.3,2X,  
&F9.3,2X,F9.3)

20 CONTINUE

10 CONTINUE

STOP

END

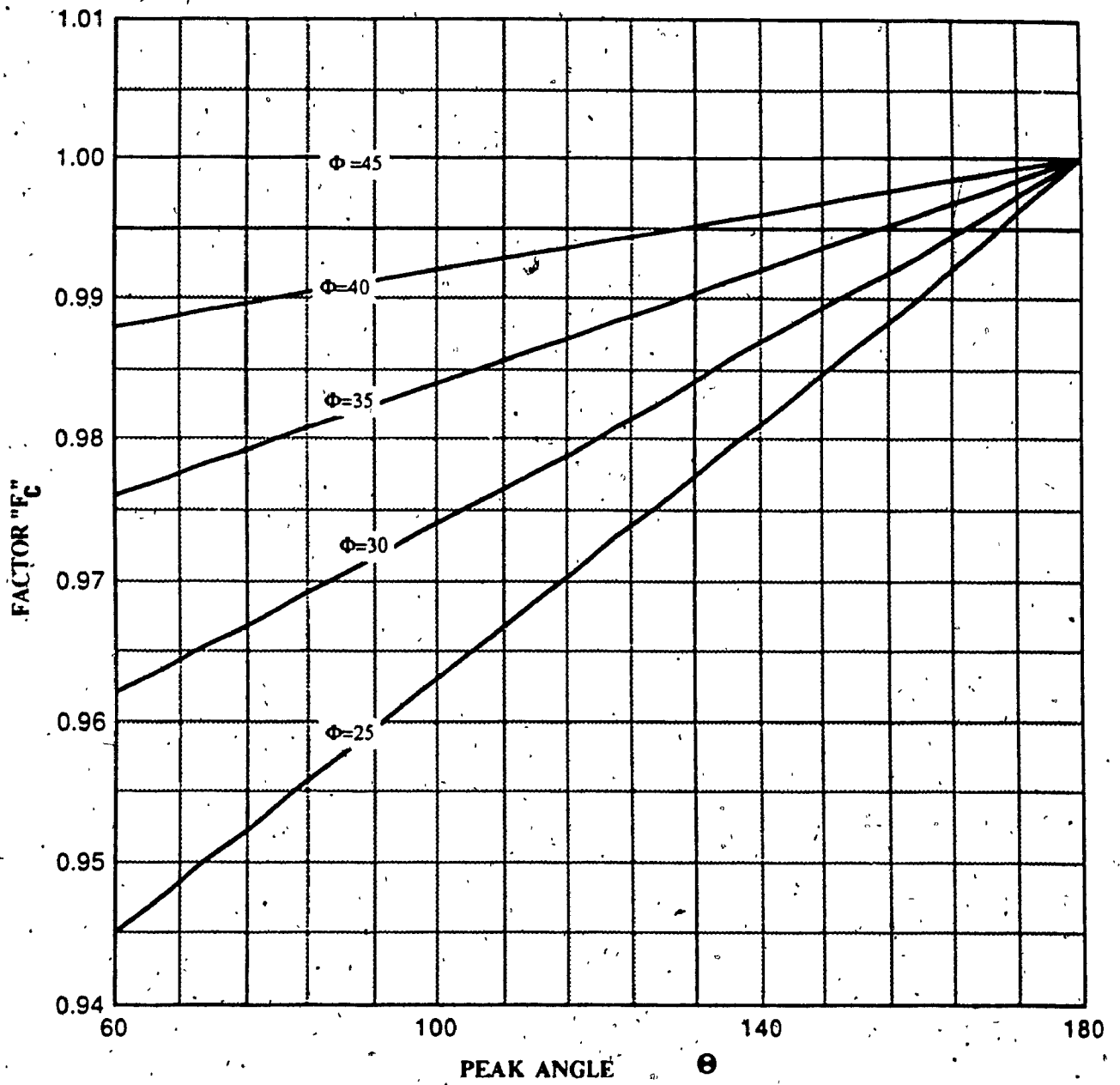


Figure 4.4 Shell Factor " $F_c$ "

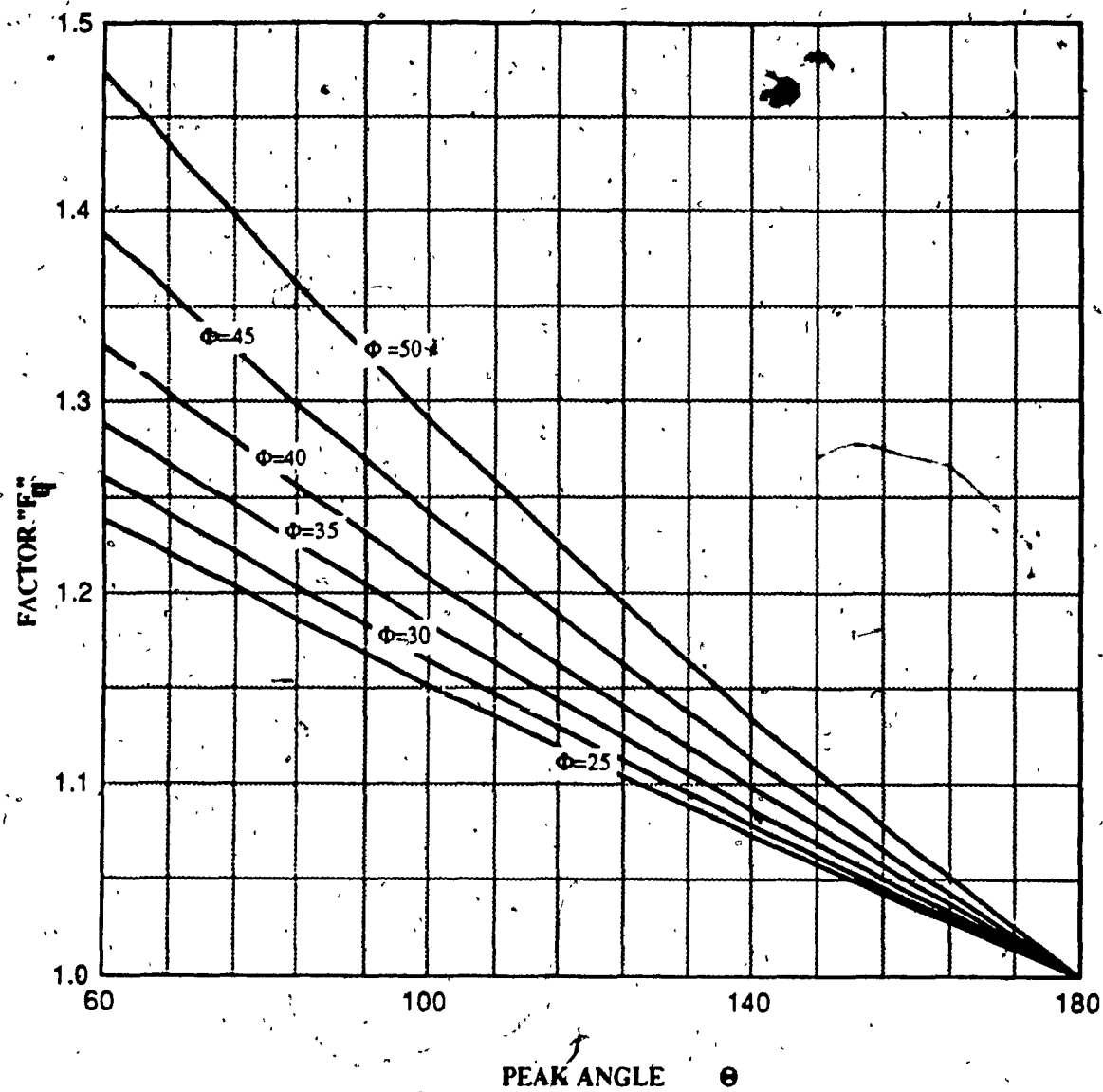


Figure 4.5 Shell Factor " $F_q$ "

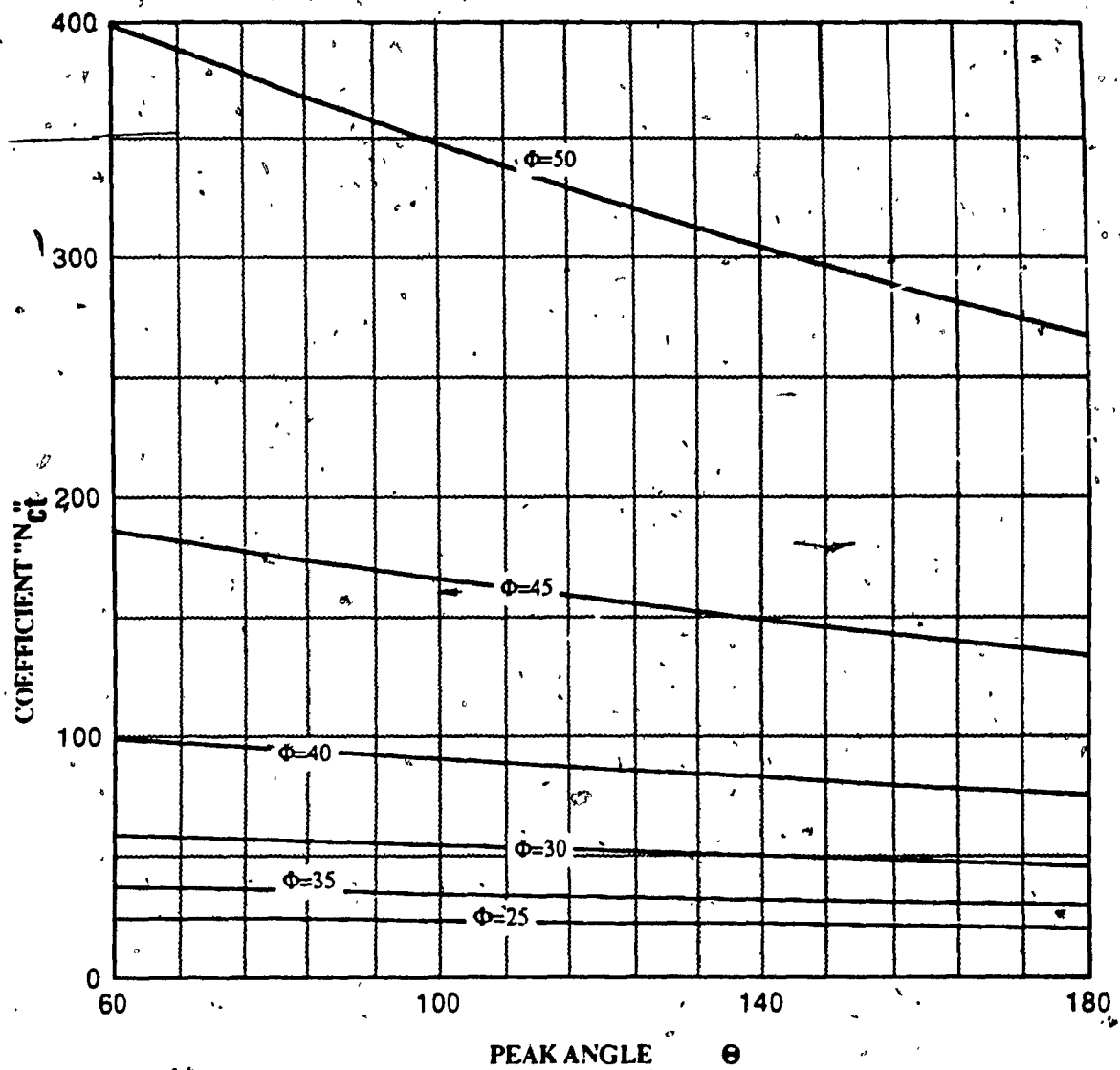


Figure 4.6 Design Chart for Triangular Strip Footing Bearing Capacity Coefficient " $N_{ct}$ "

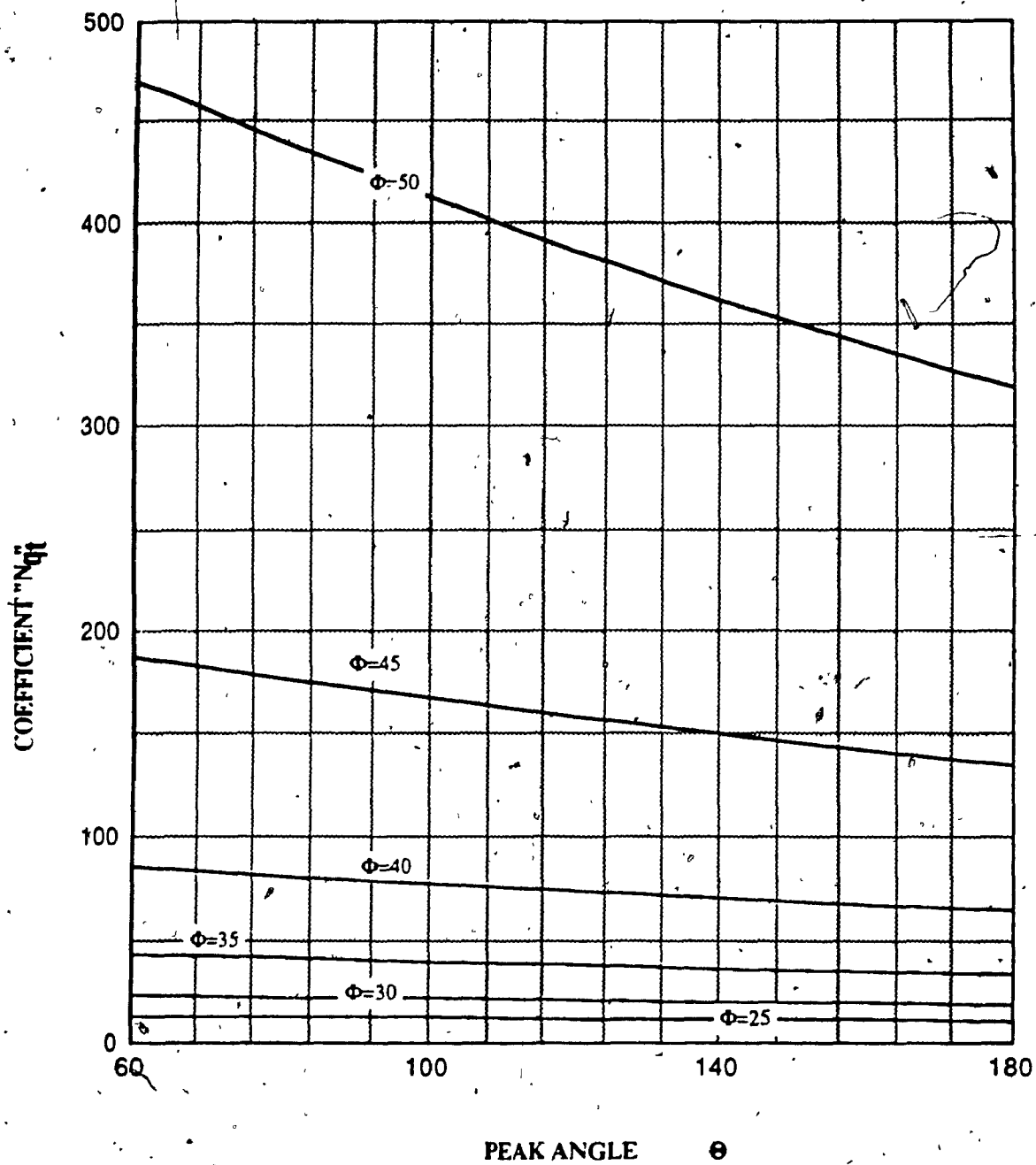


Figure 4.7 Design Chart for Triangular Strip Footing Bearing Capacity Coefficient " $N_{qt}$ "

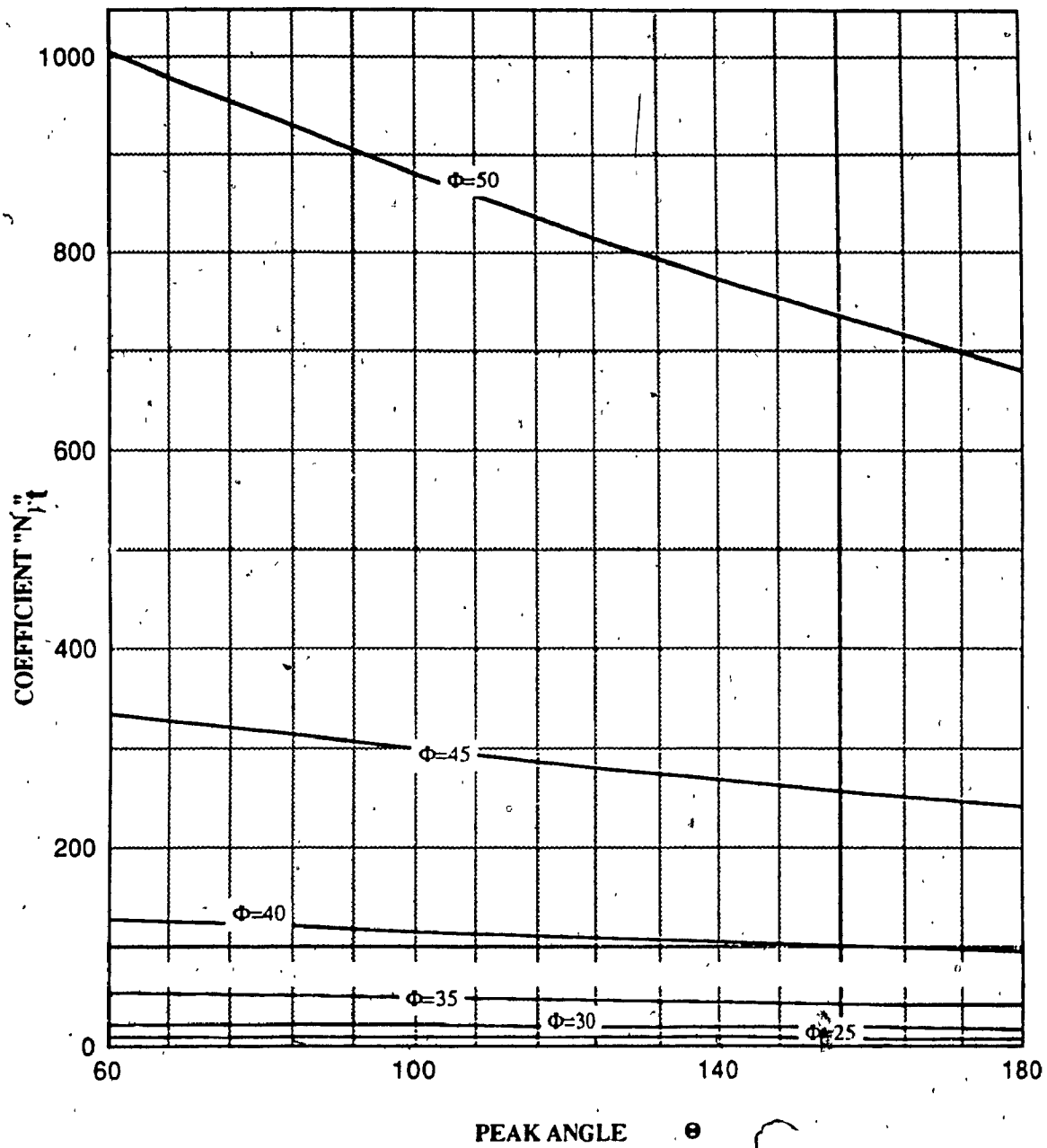


Figure 4.8 Design Chart for Triangular Strip Footings Bearing Capacity Coefficient " $N_f$ "

#### 4.4 Calculation of the Ultimate Load of the Foundation Models:

##### Common Data:

$$\gamma_{\text{sand}} = 100 \text{ lb/ft.}^3$$

$$\phi = 43^\circ \quad C = 0$$

$$B = 4 \text{ inches} \quad L = 5 \text{ inches}$$

For case of surface loading :  $D = \text{zero}$

For case of Buried Loading :  $D = 3.0 \text{ inches}$

By using equation (4.33) and the design charts for the factors  $N_{qt}$ ,  $N_{\gamma t}$  as presented in Figures 4.7 and 4.8 for the case of frictional soil, the ultimate load for each model can be calculated. The results are presented in Table 4.1 for the surface and buried loading phases. We can note that for the case of the flat footing model, i.e. peak angle  $\theta = 180^\circ$ , the factors  $F_c$  and  $F_q$  are equal to one as derived from the theoretical model and as well the coefficients  $N_{qt}$  and  $N_{\gamma t}$  will be the same as the original Terzaghi's bearing capacity coefficients. Table 4.2 presents the percentage increase of the triangular models than the flat one using the new factors according to the theory on both surface and buried loading cases.

Tables 4.3 and 4.4 present comparison between the theoretical and experimental ultimate load results for the foundation models and the results are presented in a graph in Figure 4.9 to show the validity of theory with respect to the experimental investigation.

**TABLE 4.1 THEORITICAL RESULTS FOR THE ULTIMATE LOAD FOR THE  
FOUNDATION MODELS**

Peak Angle ( $\theta$ )	Ultimate Load (lbs.)	
	Surface Loading	Buried Loading
180	380.83	724.62
140	421.75	802.11
100	467.93	889.56
90	480.58	913.52
60	520.16	988.47

**TABLE 4.2 INCREASE IN THE ULTIMATE BEARING CAPACITY OF THE  
TRIANGULAR MODELS RELATIVE TO THE FLAT ONE**

Peak Angle ( $\theta$ )	% increase in Ultimate Bearing Capacity	
	Surface Loading	Buried Loading
180	0.00	0.00
140	10.75	10.69
100	22.87	22.76
90	26.19	26.07
60	36.59	36.41



**TABLE 4.3 COMPARISON BETWEEN THE EXPERIMENTAL AND THEORITICAL RESULTS FOR CASE OF SURFACE LOADING**

Peak Angle ( $\theta$ )	Ultimate Load (lbs.)		% Difference
	Theoritical	Experimental	
180	380.83	370	+2.93
140	421.75	410	+2.87 <sup>a</sup>
100	467.93	460	+1.72
90	480.58	480	+0.12
60	520.16	520	+0.03

**TABLE 4.4 COMPARISON BETWEEN THE EXPERIMENTAL AND THEORITICAL RESULTS FOR CASE OF BURIED LOADING**

Peak Angle ( $\theta$ )	Ultimate Load (lbs.)		% Difference
	Theoritical	Experimental	
180	724.62	720	+0.64
140	802.11	800	+0.26
100	889.56	890	-0.05
90	913.52	920	-0.70
60	988.47	990	-0.15

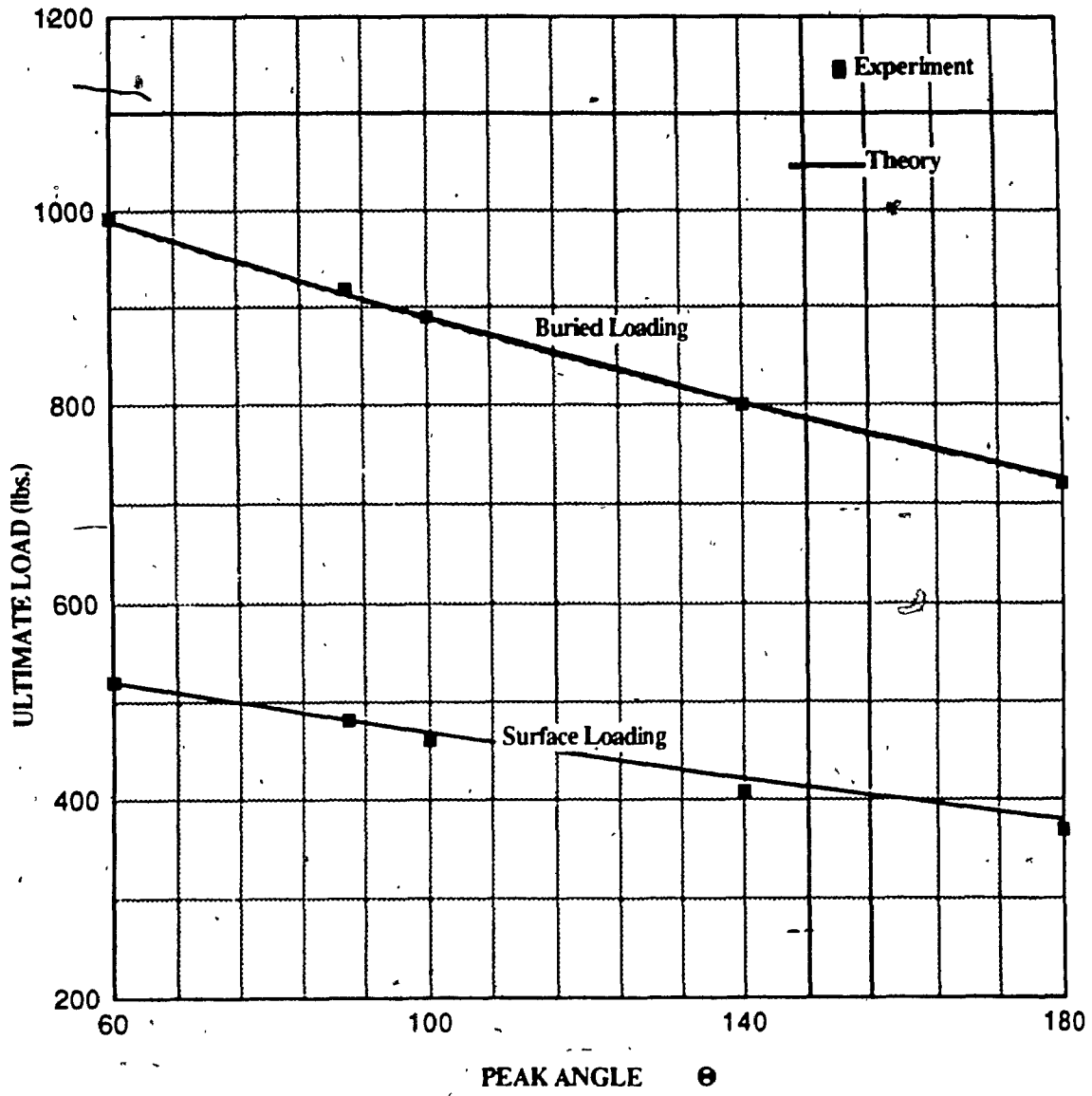


Figure 4.9 Comparison between Theoretical & Experimental Results

## CHAPTER 5

### CONCLUSIONS AND RECOMMENDATIONS

Experimental and theoretical investigations on the ultimate bearing capacity of triangular shell strip footings on sand were conducted.

In the experimental investigation five strip model footings were used. The peak angle of the foundation models varied between 180 degrees (flat type) to 60 degrees. The foundation models were tested on the surface of the sand and buried with embedment ratio of  $D/B=0.75$ . Sand placing technique and test procedure were developed. The experimental results showed that triangular strip footings, in general, have higher bearing capacity and better settlement characteristics than the similar flat foundation. It is proved also that the smaller the peak angle of the foundation, the higher bearing capacity and under the same vertical loading conditions less settlements produces. The bearing capacity of the triangular shell strip footing with peak angle equal to 60 degrees was found to be 36% more than the flat strip footing.

A theoretical model was developed by applying the theory of plasticity to simulate the failure mechanism for case of triangular strip footings. Design charts for new bearing capacity coefficients  $N_{ct}$ ,  $N_{qt}$  and  $N_{\gamma t}$  for the case of triangular strip footings were presented as functions of the angle of internal friction of sand  $\phi$  and the peak angle of the foundation  $\theta$ . Noting that these three coefficients are the same as the original Terzaghi coefficients  $N_c$ ,  $N_q$  and  $N_\gamma$  for the case of flat strip footings. By using Terzaghi's bearing capacity equation and the design charts of the new coefficients the ultimate loads for the triangular strip footings cohesionless soil can be easily predicted. It can be reported that the present experimental results are strongly support the theory developed.

Due to the common use of hydraulic powered excavators, which are capable of removing materials to very accurate tolerances and elevations, the future prospects for the excavation phase of installing triangular footings is looking more attractive. In addition, the use of Robots on construction sites is now in the experimental stage. These can be pre-programmed for excavation to very accurate shapes, elevations and tolerances, which quite conceivably in the near future can make the excavation for triangular footings a routine and economical operation.

In recent years there has been a rapid advance in the efficiency and reliability of the precast technology. This has been already adapted to conventional flat footings and the potential is there for footings of different shapes to be constructed with the same technique as well.

It can be stated that despite the fact that footings of triangular shape are more difficult and costly to construct than the flat footings, there are situations where they are technically and economically more feasible than the flat type. With new advances in construction techniques the use of shell foundations will become more technological and economical feasible.

Further reasearch should be directed to use different embedment ratios in the experimental investigation. Other shapes such as cylindrical and parabolic would be recommended for investigation as well. Triangular footings should be encouraged to come into wider use in future, wherever scope exists for employing them effectively.

## **LIST OF REFERENCES**

1. Agrawal, K.B and Gupta, R.N : "Soil - Structure Interaction in Shell Foundation", Proceedings of the International Workshop on Soil Structure Interaction, University of Roorkee, India, Nov. - Dec. 1983, Vol. I, pp. 110-112.
2. American Society for Testing and Materials Soil Specimen : "Laboratory Testing", A Symposium presented at the seventy-eighth Annual Meeting, Montreal-Canada, 22-27 June 1975.
3. Arpad, K. : "Handbook of Soil Mechanics Soil Testing", Elsevier Scientific Publishing Company, 1980.
4. Bowles, J.E.: "Foundation Analysis and Design", McGraw - Hill Book Company, Inc., 1982.
5. Chen, W.F. and Baladi G.Y. : "Soil Plasticity Theory and Implementation", Elsevier Science Publishing Company, Inc., 1985.
6. Das, B.M.: "Principles of Foundation Engineering", Brooks/Cole Engineering Division, 1984.
7. Eric, S.B.: "Model Footing Evaluation", Technical Report for Master of Eng., Concordia University, Montreal - Canada, 1987.

8. Feda, J. : "Stress in Subsoil and Methods of Final Settlement Calculations", Elsevier Scientific Publishing Company, 1978.

9. He Chong - Zhang : "Empty - Shell Foundation", The Scientific Publisher, China, 1985.

10. Kurian, N.P.: "Ultimate Strength Analysis of Shell Foundation", Proceedings of the International Workshop on Soil - Structure Interaction, University of Roorkee, India, Nov. - Dec. 1983, Vol. I, pp. 99-109.

11. Scott, C.R. : " An Introduction to Soil Mechanics and Foundations", Applied Science Publishers LTD, 1980. —

12. Selvadurai, A.P.S.: "Elastic Analysis of Soil - Foundation Interaction", Elsevier Scientific Publishing Company, 1979.

13. Terzaghi, K. : "Theoretical Soil Mechanics", John Wiley and Sons, Inc., 1959.

14. Timoshenko, S. and Goodier, J.N. : "Theory of Elasticity", McGraw - Hill Book Company, Inc., 1951.

15. Winterkorn , H.F. and Fang, H.Y. : "Foundation Engineering Handbook", Van Nostrand Reinhold Company ,1975.

## **APPENDIX "A"**

### **EXPERIMENTAL RESULTS** **Load versus Settlement**

## Cricket Graph Data

## Data(3-2)

Thu, Aug 13, 1987 7:30 PM

	LOAD(lbs)	$\theta = 180$	$\theta = 140$	$\theta = 100$	$\theta = 90$	$\theta = 60$
1	0	0	0	0	0	0
2	50	49	41	36	33	20
3	75	76	59	47	41	28
4	100	101	80	59	50	37
5	125	124	100	71	61	45
6	150	149	122	84	72	54
7	175	175	141	97	85	62
8	200	202	160	110	100	72
9	225	227	185	125	113	80
10	250	251	211	140	126	90
11	275	290	236	152	139	99
12	300	330	261	164	152	110
13	325	374	296	177	166	117
14	350	420	330	188	180	128
15	375	491	379	211	205	140
16	400	562	429	239	230	154
17	425	656	504	280	265	179
18	450	750	578	322	301	205
19	475	864	674	386	356	242
20	500	981	770	450	412	280
21	525	1090	879	537	486	329
22	550	1200	989	624	560	380
23	575	1319	1090	732	655	449
24	600	1439	1192	840	750	520
25	625	1554	1291	947	854	609
26	650	1670	1390	1055	960	700
27	675	1789	1505	1164	1075	810
28	700	1911	1621	1273	1191	921
29	725	2025	1734	1389	1300	1024
30	750	2140	1850	1506	1409	1129
31	775	2260	1971	1620	1524	1241
32	800	2380	2091	1735	1639	1355
33	825	2495	2210	1850	1754	1462
34	850	2611	2330	1965	1870	1570
35	875	2732	2448	2080	1985	1681
36	900	2851	2565	2195	2100	1790
37	0	0	0	0	0	0



## Cricket Graph Data

Data (3-3)

Thu, Aug 13, 1987 4:38 PM

	LOAD (lbs.)	$\theta = 180$	$\theta = 140$	$\theta = 100$	$\theta = 90$	$\theta = 60$
1	0	0	0	0	0	0
2	50	40	36	28	25	18
3	75	56	50	39	34	25
4	100	74	64	51	44	31
5	125	91	71	62	53	37
6	150	109	93	75	63	44
7	175	126	107	87	72	51
8	200	144	123	99	82	57
9	225	161	139	110	92	63
10	250	179	153	122	102	70
11	275	197	168	135	112	77
12	300	215	182	147	122	84
13	325	232	197	160	132	91
14	350	251	212	172	143	99
15	375	269	227	184	151	106
16	400	287	242	196	162	113
17	425	305	257	209	172	120
18	450	323	272	221	181	126
19	475	341	286	233	190	132
20	500	360	300	245	200	139
21	525	384	319	257	209	145
22	550	409	338	270	219	152
23	575	449	369	285	229	158
24	600	489	400	300	240	165
25	625	535	431	320	264	181
26	650	581	462	341	291	200
27	675	615	506	373	315	216
28	700	649	551	407	340	235
29	725	739	599	449	370	267
30	750	830	649	492	401	301
31	775	927	720	542	445	337
32	800	1025	792	593	492	375
33	825	1158	856	640	544	421
34	850	1290	920	680	597	470
35	875	1440	1030	740	657	514
36	900	1590	1142	830	720	560
37	925	1740	1272	920	804	614
38	950	1891	1403	1010	891	670
39	975	2041	1559	1134	995	744
40	1000	2191	1717	1258	1100	820
41	1025	2341	1873	1408	1266	910
42	1050	2493	2030	1560	1433	1000
43	1075	2643	2186	1728	1599	1098
44	1100	2794	2344	1896	1767	1198
45	1125	2944	2500	2064	1933	1350
46	1150	3094	2659	2232	2102	1502
47	1175	3245	2816	2399	2289	1650
48	1200	3396	2974	2567	2435	1798
49	1225	3546	3131	2735	2601	1998
50	1250	3696	3288	2904	2768	2200
51	1275	3846	3444	3072	2935	2401
52	1300	3996	3603	3240	3103	2602
53						
54						